André Tiago Carreira e Silva

Sistema Remotamente Alimentado para Redes Ópticas Passivas

Remote Powered System for Passive Optical Networks

André Tiago Carreira e Silva

Sistema Remotamente Alimentado para Redes Ópticas Passivas

Remote Powered System for Passive Optical Networks

Dissertação apresentada à Universidade de Aveiro para cumprimento dos requisitos necessários à obtenção do grau de Mestre em Engenharia Electrónica e Telecomunicações, realizada sob a orientação científica do Dr. António L. J. Teixeira, do Instituto de Telecomunicações e do Departamento de Electrónica, Telecomunicações e Informática, e do Dr. Rui M. Escadas, do Departamento de Electrónica, Telecomunicações e Informática, da Universidade de Aveiro.

Dedicatória

Dedico este trabalho aos meus pais pela paciência, apoio e pelos puxões de orelhas dados ao longo destes anos de formação Superior, e a toda a minha família e amigos pelo ombro amigo naqueles momentos menos bons pelos quais todos nós passamos.

Quero ainda dedicar a todos os meus amigos universitários que me acompanharam nesta etapa da minha vida, e nas inúmeras aventuras e desventuras desta minha passagem pela Universidade de Aveiro.

O Júri / The Jury

Presidente	Prof. Dr. José Rodrigues Ferreira da Rocha Professor Catedrático do Departamento de Electrónica, Telecomunicações e Informática da Universidade de Aveiro
Orientador	Prof. Dr. António L. J. Teixeira Professor do Departamento de Electrónica, Telecomunicações e Informática da Universidade de Aveiro
Co-Orientador	Prof. Rui Manuel Escadas Ramos Martins Professor Auxiliar do Departamento de Electrónica, Telecomunicações e Informática da Universidade de Aveiro e Membro do Instituto de Engenharia Electrónica e Telemática de Aveiro.
Convidado	Dr. Ruben Soares Luís Investigador no Centro de Vulcanologia da Universidade dos Açores

Agradecimentos / Acknowledgements

Expresso desta forma a minha gratidão para com o meu orientador, Dr. António Luís de Jesus Teixeira, pela oportunidade que me foi dada ao me entregar este trabalho para execução, ao meu Co-Orientador Dr. Rui Manuel Escadas Ramos Martins, pelo incansável apoio, preocupação, ajuda e extrema paciência que demonstrou durante estes longos meses de trabalho, e a todos os colaboradores com quem me cruzei durante a realização deste trabalho, nomeadamente o Engenheiro André Quinta e o Engenheiro Rodolfo Andrade, por todas as respostas e orientações dadas ao longo do projecto.

Aproveito também para deixar aqui um especial agradecimento ao meu Padrinho e amigo Ricardo Rodrigues que sempre se mostrou disponível para ajudar e apoiar quando necessário.

Gostaria igualmente de expressar a minha gratidão para com toda a minha família, em especial aos meus pais, Isidro Silva e Maria José Silva, por toda a paciência, confiança e força depositadas em mim durante todos estes anos de Universidade, não sei o que seria de mim sem eles, para eles um grande 'Obrigado por Tudo!'.

Por último um grande agradecimento a todos os meus amigos e companheiros de curso com quem me cruzei nestes anos de Academia, sem eles, e elas, não teria havido aquela magia da confraternização que só eles sabem dar!

Palavras-chave

Comunicações Ópticas, Redes Ópticas Passivas de Nova Geração, Alimentação Remota, Alimentação por Fibra Óptica, Nó Remoto.

Resumo

As redes passivas são cada vez mais uma realidade. Os standards estão a desenvolver-se rapidamente (NG-PON, G-PON, etc), e cada vez mais o consumidor final tem maior necessidade de largura de banda, que, numa primeira fase, irá certamente, ser distribuída por redes passivas integralmente ópticas. As redes passivas são, por si, uma solução interessante para os operadores, pois, sendo passivas minimizam os custos de manutenção. No entanto, o reverso desta passividade e transparência, é que estas podem ser alteradas por simples aumento do número de ramais de uma forma independente e potencialmente incontrolada. Um aumento do tráfego, bem como um crescente de procura de novos serviços e larguras de banda, vêm forçar o desenvolvimento de novas tecnologias que permitam um redimensionamento e redefinição da rede, nomeadamente nós ópticos transparentes. O objectivo principal deste trabalho é estudar os processos de alimentação remota de sistemas de comutação e reconfiguração para utilização em redes ópticas passivas, e fazer uma implementação de alguns modelos para teste.

De salientar que este projecto enquadra-se no projecto Europeu “SARDANA” e nas redes de excelência “BONE” e “Euro-FOS”.

keywords

Optical Comunications, New Generation Passive Optival Networks, Remote Power, Power Over Fiber, Remote Node.

abstract

The passive networks are becoming a reality. The Standards are evolving rapidly (NG-PON, G-PON, etc), and now, the consumer, more than ever, has a major necessity for bandwidth, which, in a first stage, will certainly be distributed by fully passive optical networks. The passive networks are, on their own, an interesting solution for operators, because, being passive, minimize the maintenance costs. However, the other side of the passiveness and transparency is that it can be altered by simple increase of the number of branches in a independent way and potentially uncontrolled. An increase of traffic, as an increasing search of new services and bandwidth, are forcing the development of new technologies which will allow a network resizing and redefinition, in particular, the transparent optical nodes. The main objective of this work is study the remote powering processes for commutable and reconfigurable systems, to be used in passive optical networks, and implementing some models for testing.

Note that this Project falls within the European project “SARDANA” and in the networks of excellence “BONE” and “Euro-FOS”.

Index

List of Figures

List of Acronyms

ALD
Analog Linear Devices 35, 36, 38, 39, 42, 46
APD
Avalanche Photo Detector 17
C
Celsious Degree 34
CMOS
Complementary Metal Oxide Semiconductor 4, 5
CO
Central Office 7, 22, 23
DC
Direct Current ... 2, 9, 11, 12, 13, 14, 19, 24, 25, 29, 34, 35
DTMOS
Dynamic Threshold Metal Oxide Semiconductor 5
EH
Energy Harvesting 15, 16, 17, 25
EMI
Electromagnetic Interference 13
EPAD
Electrically Programmable Analog Device 35, 36, 39
FET
Field Efect Transistors 13
FTTH
fiber-to-the-home 20
Ge
Germanium 17
GPR
Ground-Potential Rise 32, 33
IC
Integrated Circuit 14, 49, 87
I_{ds}
Drain to Source Current 44
Indium Gallium Arsenide 17
IPTV
Internet Protocol Television 6
kHz
kilo Hertz 13
LED
Light Emitting Diode 34
mA
milliAmp 25, 26, 28, 30, 34, 35
MOSFET
Metal Oxide Semiconductor Field-Effect Transistor 25
Metal Oxyde Semiconductor Field Effect Transistor 35, 36, 37, 39, 44, 46
MOSFETs
Metal Oxide Semiconductor Field-Effect Transistor 34, 35, 38
MT-CMOS
Multi-Threshold Complementary Metal Oxyde Semiconductor 5
mV
milliVolt 14, 19, 27, 28, 30, 34, 35
mW
milliWatt 34
nA
nanoAmp 25, 29
NG-PON
New Generation Passive Optical Network 5, 20
NiCd
nickel-cadmium 26
NiMH
nickel-metal hydride 26
nm
nanometer 33
ORN
Optical Remote Node 5
OS
Optical Switch 9
PCB
Printed Circuit Board 65
PDA
Personal Digital Assistants 4
PIC
Programmable Interrupt Controller 9, 34
PICs
Programmable Interrupt Controllers 8

List of Tables

Chapter 1: Introduction

1.1 Context

Since the beginning the Human Kind, the energy demand has increased. Nowadays, this increase, due to the modern industrial society and population growth, and the interest in the environmental issues that helped to raise the effort to find new sources of energy to allow reduction in the utilization of the natural resources of fuel and to improve energy efficiency and power quality issues. Within this context, the renewable energies, like the solar or wind energy appear as an important, and most reliable, alternative to the increase of the energetic consumption of the planet.

The renewable energy options are viable and just to give an idea of the potential of this sort of renewable energy. Take, for example, the solar energy, since there are large desert areas, or areas located in tropical and temperate regions, where the direct solar density may reach up to 1 Kw/m2. Photovoltaic (PV) generation is gaining increased importance as renewable source due to some of its major characteristics, such as sunlight that can be converted directly into electrical power, with low maintenance, no noise and no pollution.

The photovoltaic technology can be obtained from all light wavelengths and sources, such as ultraviolet, infrared or even the most common denominated visible light. Some useful applications that take advantage of this technology are, for instance, solar panels used for all sort of things, like traffic signals or emergency highway phones. Yet in terms of light, photovoltaic technology and some of its applications, for example, communications, one of the main areas relate to fiber optics. It is one example of a communication

technology involving light. This communication technology adds low noise, is able to perform high speed and is robust to electro-magnetic external noise.

Combining the fiber optic communication and the photovoltaic technology, we will observe means to transmit Power over Fiber, (PoF). Almost all modern digital systems are supplied with power through power lines or batteries, however there are some types of devices that need to be placed in hazardous or unreachable places that need to be fed by other means. Those are some of the situations addressed by PoF and this document.

PoF is a technology that allows providing power through an optical fiber, thus removing the need to have extra copper wires or other type of power cables, as it continues to transport the data as a normal network. This technology is normally associated with Passive Optical Networks (PON).

In any case, the energy levels involved are low due to the fiber characteristics (small core area, which would burn if high power is fed (1). To collect these negligible power levels, low power electronics is required. As all low or ultra low power electronics, the remote nodes where the PoF is enabled are supplied with power stemming from photodiodes, that convert the optical signal in to electrical power, and DC-DC converters, that should be high performance devices and optimized to specific supply voltage ranges.

Regarding the DC–DC converters, they should be high performance devices due to the low or ultra low voltages that are involved, some minimum typical values are between 3 or 3.3 volts (2) (3), in their main function which is to transform a generally low or ultra low input voltage into something useful. A DC-DC converter is a class of switching-mode power supply (SMPS).

For high performance and high efficiency, the SMPS must run at high rates and have low losses. The advent of a commercial semiconductor switch in the 1950's represented a major milestone that made SMPSs such as the boost converter, the heart of a DC-DC converter, possible. Semiconductor switches turned on and off more quickly and lasted longer than other switches such as vacuum tubes and electromechanical relays. The major DC to DC converters were developed in the early-1960s when semiconductor switches had

become available. The aerospace industry's need for small, lightweight, and efficient power converters led to the converter's rapid development.

Switched systems such as SMPS are a challenge to design since its model depends on whether a switch is opened or closed. R.D. Middlebrook from Caltech (California Institute of Technology) in 1977 published the models for DC to DC converters used today. Middlebrook blended the circuit configurations for each switch state in a technique called state-space averaging. This simplification reduced two systems into one. The new model led to insightful design equations which helped SMPS growth (4) (5).

DC-DC converters are generally classified into two types, namely: 1) linear voltage regulators and 2) switching voltage regulators, according to the circuit implementation type. However, nontrivial power dissipation is unavoidable in both types of voltage conversion and that directly affects the battery life. The amount of lost energy, due to nontrivial power losses, is almost 10% to 40% of the total energy consumed in the system..

It is generally known that switching regulators achieve better power efficiency than linear regulators, but linear regulators are much cheaper and produce less noise than switching regulators. For this reason, switching regulators are mostly used for low power or high-current application, except when low noise or low cost is particularly important.

Since these converters are small, with tendency to become smaller, light weighted, with high efficiency, they are the ideal component for a PoF project. We will be working with ultra low voltages and these converters are ideal to boost them up to values that can be used to power up the other available hardware that need more voltage that the one that was available at the first place. This DC-DC conceit will contribute not only for this PoF project but will also be useful for other type of technology that has low or ultra low input voltages.

1.2 Motivation

There is a growing need for low and ultra low power for example in our pockets or in our office, from our mobile phone or Personal Digital Assistants (PDAs) to our laptop or netbook, everything needs batteries to work. Some sorts of batteries are not environmentally friendly, as there are some compounds that are extremely toxic and dangerous to animals and plants. These compounds should be in all cases avoided. To solve these types of problems, people have turn themselves to renewable energies and non-polluting sources of power. However, the main issue, and the main reason that moved my interest to this work was the fact that those types of energy are available in very low quantities, and to be used, they need to be efficiently harvested and stored.

The devices and technologies that require external voltage sources, like batteries or some sort of harvesting technique, are growing at a high rate. There are statistics that show a strong growth of cell phone selling's and subscriptions (6). A cell phone is a device that works with batteries, and it is known that the normal batteries do not have the necessary voltage to work with all the electronic inside a portable terminal, that is why it needs to be leveled up to a more useful voltage, by a step-up technique.

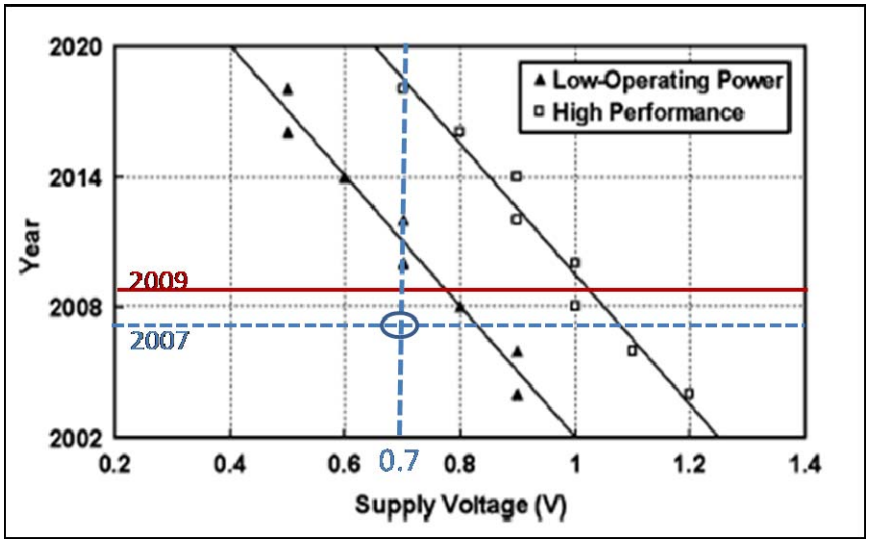

Figure 1 - Forecast of the CMOS supply voltage by International Technology Roadmap for Semiconductors (ITRS) 2004 (7); The circle point marks the Schmitt Trigger developed by Kyung Ki Kim and Yong-Bin Kim in 2007(8).

Figure 1 shows us a forecast of the CMOS supply voltage, where a low-voltage operation of 0.4 V is anticipated by the end of 2019. Therefore, it instigates the development of low-voltage circuit techniques for high-performance Integrated Circuits. It can be seen that the graphic is outdated, as the line that represents the 2009 year shows that in the present year the CMOS supply voltage should be about 0,8 V and that does not correspond to the truth, because there already are devices using CMOS technology working below that supply voltage. For instance, there is a Schmitt Trigger developed by Kyung Ki Kim and Yong-Bin Kim in 2007 (8), that considers an ultra-low voltage and high speed designed in silicon-on-insulator (SOI) technology. The proposed circuit is designed using dynamic threshold MOS (DTMOS) technique and multi-threshold voltage CMOS (MT-CMOS) technique to reduce power consumption and accomplishes high speed operation. The experiment shows the proposed Schmitt trigger circuit consumes 4.68μW at 0.7V power supply voltage, marked as a traced line in Figure 1, and the circuit demonstrates the maximum switching speed of 170psec (8). It can be observed in the graphic that the Schmitt Trigger, in 2007, was way ahead of the prognostic of the graphic since it only predicted the supply voltage of 0,7V around year 2011.

Some other typical applications using low or ultra low voltage sources are those that have some sort of harvesting technique. One of the main applications, and where this document is focused, is the power source of an optical Remote Note (ORN or RN), a base component of a New Generation of Passive Optical Network (NG-PON).

There is a growing need for bandwidth driven for the demand from residential and business users (9). It causes a demand from the scientific community for infrastructures that support large scale data transport and processing. In Figure 2 it can be seen that the capacity of the optical network has increased exponentially over the years. These bandwidth demands are mainly driven by IP traffic which now includes IP video that have migrated from the initial closed IPTV to a more open internet based model and intensive transaction web 2.0 applications. A good example is the current service known as triple play, which includes

not only the normal internet services, but also phone services, like Voice Over Internet Protocol (VOIP), and high definition TV, like Internet Protocol Television (IPTV).

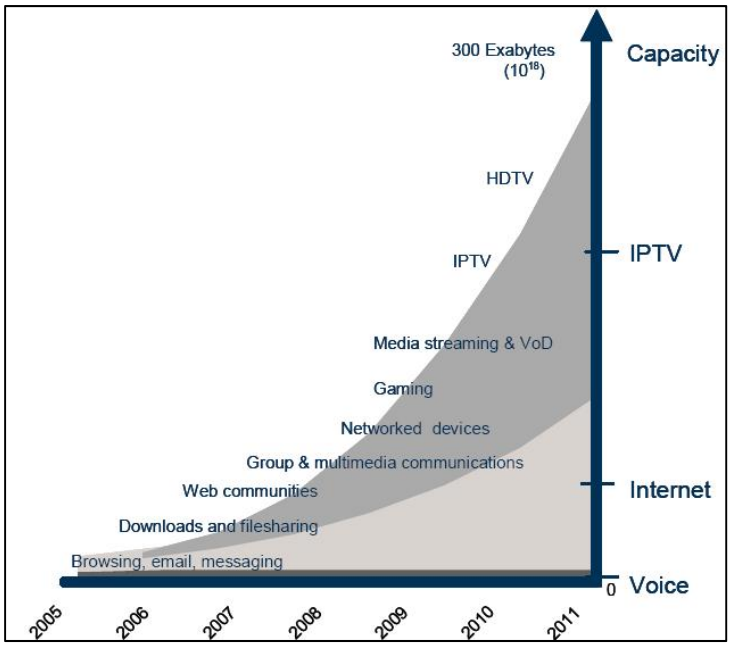

Figure 2 - Forecast subscriber services/capacity to 2011(9)

These new services demand that the communication channels can support high speed data transfers, and the best way to provide such high speed is through optical fiber.

Being the optical fiber networks already a reality, they are required to become faster, more complex and more advanced. The next logical step in the evolution of the optical networks is making them greener and less dependent on external sources of energy. The passive optical networks (PON) are an example of that- The main advantages of these networks are the lower maintenance costs (passive) and higher transparency.

An example of that type of networks is the project Scalable Advanced Ring Based Passive Dense Access Network Architecture, also known as SARDANA.It consists of a Metro-Access convergence network able to supply at least 100Mb/s to 1024 users spread over more than 100Km. In Figure 3 is presented the main structure of SARDANA.

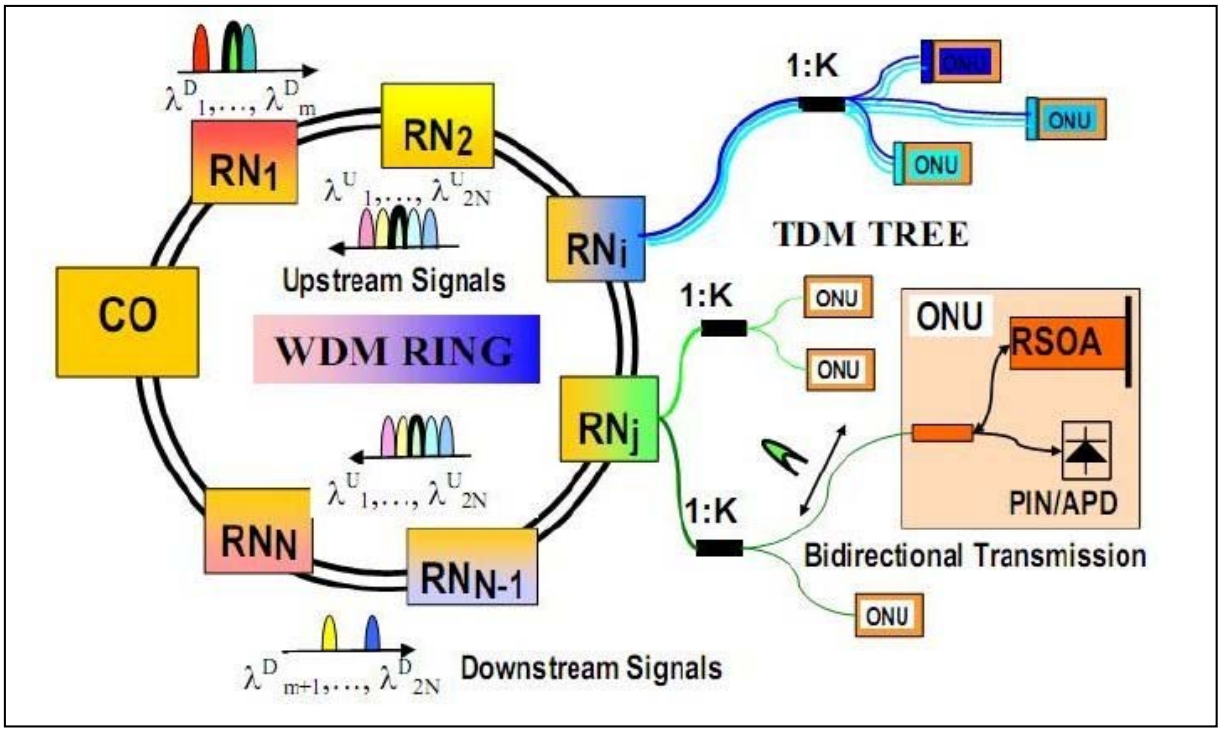

Figure 3 - a) SARDANA network architecture(10)(11)

Robustness in this optical network is achieved by the passive ring, monitoring techniques and compensation strategies intelligently supervising and managing the impairments of the PON. Due to the ring, the network is able to provide traffic balance through the shorter path and resiliency in case of fiber, splice, connector or component failure, being the signals redirected to the alternative path.

The SARDANA network scalability is guaranteed by inserting supplementary remote nodes (RN) to the ring that is wavelength transparent. The network can be scaled to reach a large number of subscribers.

As can be seen in Figure 4, the remote nodes establish the connection between the double-fiber ring and the single-fiber-trees and are able to Add&Drop and distribute to each access tree the assigned wavelengths being transparent to the other WDM channels on the ring. The RNs are able to compensate distance from the CO, Add&Drop and filtering losses providing gain by means of EDFs, remotely pumped from the CO. Simple Optical Network

Unit (ONU) implemented with a colorless Reflective Semiconductor Optical Amplifier (RSOA) provides upstream (US) re-modulation at the same wavelength as for the DS signal (12).

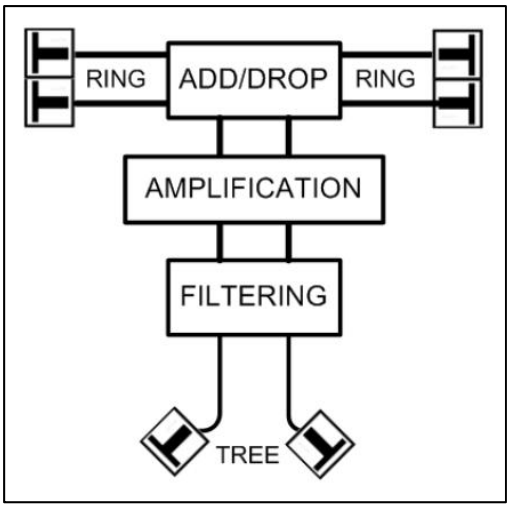

Figure 4 - Remote Node main Structure

A RN is an important component of the SARDANA network and it needs a special attention given to all its internal components, mainly its power source. The RN is a part of the passive optical network, which means that there is no electricity supply. All the internal hardware needs to harvest the energy that circulates in the optical fiber, mainly light, stores it and uses it to operate the internal hardware, such as optical switches and Programmable Interrupt Controllers, PICs. This document is about the power source, the harvesting technique and storage system.

The main work challenge relates to the unavailability of a solution for an ultra low power remote node fed by light.

1.3 Structure and Objectives

This document is divided in five chapters, all related with low or ultra low voltage systems, their main parts explanation and implementation. There is also an overview about commercial circuits with some explicit characteristics, tests, results and some conclusions about them.

In this first chapter it is presented the context of the work and its main objectives together with the structured description of each chapter.

The second chapter offers the State of the Art that describes the main utilizations and characteristics of the low or ultra low voltage Sources. An introduction to the new technology called Power over Fiber (PoF), and an evaluation of existing commercial solutions from Texas Instruments, ST Microelectronics and from Advanced Linear Devices is also presented.

The Third chapter describes PoF technology, where it is applied, and it gives a more detailed description about the problem. It introduces the Ultra Low Voltage Source as a DC-DC system that can transform 0.4 volts, harvested from an optical fiber, through a PIN photodiode, into a value needed to feed all the electronics inside a remote node, like Programmable Interrupt Controllers (PICs) or Optical Switches (OS) (Solution found in this work).

In Chapter Four, every single block introduced in the Third chapter is explained with detail, and all the problems encountered during the implementation are presented. Also all components used to create the final block are introduced, explained and tested. Tests to all blocks and to the system and some conclusions are also presented.

The Fifth Chapter introduces a Germanium based approach. This approach uses bipolar germanium transistors and a dual boost technique to achieve the necessary output to work with the internal hardware regarding the current consumption.

Finally, in the Sixth Chapter, presents some final conclusions, and suggests some guidelines for a future work to improve the final system.

1.4 Main Contributions

In the author's opinion, the main contributions of this work may be summarized as follows:

- Understanding the need for ultra low voltage sources in fiber optics networks, due to maintenance or placement;
- Design of a 0,4 V, or lower, operating subsystem
- Extensive state of the art:
    - Evolution of low or ultra low voltage sources;
    - DC-DC converters;
    - Energy Harvesting;
    - Power Over Fiber Technology;
    - PON, more precisely Remote Nodes and the available solutions;
    - Commercial Low or Ultra Low Voltage sources and Harvesting Modules;
    - Evaluation of the existing commercial Low or Ultra Low Voltage Sources and Harvesting Module;
- Provide an extensive description about a new type of an ultra low voltage circuit, beginning with the oscillator, going through the Boost and finally, the storage system;
- Describe germanium technology, in particular the Bipolar Germanium transistors;

Chapter 2: State of the Art and Evaluation of Existing Solutions

2.1 Evolution of the Low Voltage and Ultra Low Voltage Sources

Following the effort leaded by pro-environment organizations, fighting for a better planet against pollution and other things harmful to our planet, like coal or petroleum, used to create energy, people started to search for new types of renewable sources of energy. Those types of energy, like the solar or eolic energy, for example, need to be transformed, and maybe stored, before they can be correctly used. The major's impediments to the use of these new energy types are the special devices needed to capture and harvest.

All the energy is intended for industrial or home use, as well as some applications requiring very little energy, for example, little garden lamps, road signs, highway emergency phones or even parking meters. Those kinds of devices can, by themselves, collect and store the energy amount for its needs. Sometimes the energy that is harvested from the sun or whatever energy source does not always has the proper voltage to be used and needs to be lowered or to be pulled up according to the specific situation. This is one of the main objectives of this work, to raise a low voltage into a higher voltage level, good enough to be used or stored.

The search for low power or low voltage sources started when the radio frequency (RF) technology appeared. It was a new technology intended to control or monitor devices wirelessly so that these devices should consume very little energy. In the area of the low or ultra low voltage sources, very few are intended for input voltages below 1 volt. It is imperative, when working with low or ultra low voltage sources, to refer DC-DC converters. These devices are an electronic circuit which converts a source of direct current (DC) from

one voltage level to another (it is a class of power converter). DC to DC converters are important in portable electronic devices such as cellular phones and laptop computers, which are supplied with power from batteries primarily. Such electronic devices often contain several sub-circuits, each with its own voltage level requirement different than that supplied by the battery or an external supply (sometimes higher or lower than the supply voltage, and possibly even negative voltage). Additionally, the battery voltage declines as its stored power is drained. Switched DC to DC converters offer a method to increase voltage from a partially lowered battery voltage thereby saving space instead of using multiple batteries to accomplish the same thing.

DC-DC converters have three types of conversion methods:

Linear

This type of regulators can output a lower voltage from the input. They are very inefficient if the voltage drop is large and the current high as they dissipate as heat power equal to the product of the output current and the voltage drop; consequently they are not normally used for large-drop high-current applications.

However, one of the advantages is if the current is low, the power dissipation is also low, although it may still be a large fraction of the total power consumed.

Linear regulators are inexpensive, reliable if good heat sinking is used and much simpler than switching regulators. As part of a power supply they may require a transformer, which is larger for a given power level than that required by a switch-mode power supply. Linear regulators can provide a very low-noise output voltage, and are very suitable for powering noise-sensitive low-power analog and radio frequency circuits. A popular design approach is to use an LDO, Low Drop-out Regulator, which provides a local "point of load" DC supply to a low power circuit.

Switched-mode Conversion

These types of converters convert one DC voltage level to another by storing the input energy temporarily and then releasing that energy to the output at a different voltage. The storage may be in either magnetic field storage components (inductors, transformers) or electric field storage components (capacitors). This conversion method is more power efficient (often 75% to 98%) than linear voltage regulation (which dissipates unwanted power as heat). This efficiency is beneficial to increase the running time of battery operated devices. The efficiency has increased in since the late 1980's due to the use of power Field Effect Transistors (FETs), which are able to switch at high frequency more efficiently than power bipolar transistors, which have more switching losses and require a more complex drive circuit. Another important innovation in DC-DC converters is the use of synchronous switching which replaces the flywheel diode with a power FET with low "On" resistance, thereby reducing switching losses.

The disadvantages of these switching converters include complexity, electronic noise (EMI / RFI) and to some extent cost, although this has come lower with advances in chip design.

Magnetic

In these DC to DC converters, energy is periodically stored into and released from a magnetic field in an inductor or a transformer, typically in the range from 300 kHz to 10 MHz. By adjusting the duty cycle of the charging voltage (that is, the ratio of on/off time), the amount of power transferred can be controlled. Usually, this is done to control the output voltage, though it could be done to control the input current, the output current, or maintain a constant power. Transformer-based converters may provide isolation between the input and the output. In general, the term "DC to DC converter" refers to one of these switching converters. These circuits are the heart of a switched-mode power supply.

A good example of a DC-DC magnetic converter is a boost converter. This step-up converter is a power converter with an output DC voltage greater than its input DC voltage. It is a class of switching-mode power supply (SMPS) containing at least two semiconductor

switches (a diode and a transistor) and at least one energy storage element. For high efficiency, the SMPS switch must turn on and off quickly and have low losses.

As good examples of technologies or applications that use low or ultra low power from natural sources, that need or use the DC-DC converters, we have a Self-Powered Low Power Signal Processing (13) that is a chip that has been designed and tested to demonstrate the feasibility of operating a digital system from power generated by vibrations in its environment, other system is Stand-Alone Photovoltaic Energy Storage System With Maximum Power Point Tracking (14), this work deals with the study of a stand-alone photovoltaic system, which is able to extract the maximum power from photovoltaic array for all solar intensity conditions and to provide output voltage regulation. It is a system composed by a dc-dc converter in combination with battery energy storage in a simple structure. And as a final example we have an Energy Harvesting for Wireless Communication Systems Using Thermo generators (15), which is an energy harvesting circuit that supplies power to a wireless communication module for transmitting sensor data to a receiver. A thermo generator module (TEG) is employed to harvest energy from temperature gradients between a heat source, e.g. the human body, and the ambient. The output of the TEG is connected to a step-up dc-dc converter to increase the available voltage in order to supply a wireless communication module and to charge an energy storage element. A startup IC is employed to power-up the switch-mode dc-dc converter (16)(17)(18)(19).

2.2 Energy Harvesting

Traditionally, electrical power has been generated in large scale and provided in sufficient amounts, but ambient energy, such as sun, wind and tides, which are widely available have no technologies with high efficiency to capture it. Energy harvesters currently do not produce sufficient energy to perform mechanical work, but instead provide very small amount of power for powering low-energy electronics. While the input fuel to large scale generation costs money (oil, coal, etc.), the "fuel" for energy harvesters is naturally present

and is therefore considered free. For example, temperature gradients exist from the operation of a combustion engine and in urban areas and there is also a large amount electromagnetic energy in the environment due to radio and television broadcasting.

Energy Harvesting (EH) is the process of capturing energy from any energy source, store that energy, conditioning it into a form that can be used later, for instances to operate a microprocessor within its operating limits, or any other type of electronic controllers. In many common cases, EH is associated with capturing residual energy as a by-product of a natural environmental phenomenon or as a by-product of industrial processes. Often these residual energies were not previously captured, but instead were released into the environment as waste. Common target energy harvesting sources for EH are mechanical energy resulting from vibration, stress and strain; thermal energy from furnaces and other heating sources, even biological; solar energy from all forms of light sources, ranging from lighting, light emissions and the sun; electromagnetic energy that are captured via inductors, coils and transformers; wind and fluid energy resulting from air and liquid flow; and chemical energy from naturally recurring or biological processes.

In most cases, these sources provide energy in very small packets that have been difficult to capture for use. New opportunities in Energy Harvesting are being enabled by new EH circuits that can finally provide the overall Energy Management to capture and store these small energy packets and condition them to provide a useful output. The Energy Management provided by these EH circuits need to include high **Energy Efficiency** to capture and accumulate these small energy packets; high **Energy Retention** to store the energy for long periods of time; and the proper **Energy Conditioning** to perform the desired task. The Energy Conditioning must be well defined even starting at 0.0V operation and tolerate a wide range of voltage, current, and waveform inputs, including over-voltage, over-charge, and other irregular input conditions(20).

- **Energy Efficiency**

The Energy Management of capturing, accumulating and storing small packets of electrical energy requires High Energy Efficiency. The net captured energy is a direct function

of energy available for capture minus the energy the EH circuit must consume to stay in the active mode. The circuit must stay in the active mode and be ready to perform the energy capture whenever harvestable energy becomes available and be ready to provide an output as the application design requires it. For example, let's say the energy is vibration from someone walking on a surface embedded with a vibration energy source with an EH circuit and a temperature sensor and wireless transmitter. The small energy packets provided from the possibly infrequent pedestrian must power the EH circuit in the active mode for a long period of time until the EH circuit triggers the transmitter to send the temperature data. The Energy Efficiency must be very high so that the energy consumed by the EH circuit is much smaller than the small energy provided by the vibrations.

- **Energy Retention**

A second key component of Energy Management is High Energy Retention to store the captured energy for as long as possible with minimal leakage or loss. In the example of the pedestrian, if pedestrian activity is low, it may be many hours before enough energy has been stored by the EH circuit to trigger the data transmission or many hours before the application design wants the data transmitted. Therefore, the EH circuit must have extremely high Energy Retention.

- **Energy Conditioning**

This is the third key component of Energy Management. The EH circuit must Condition the stored energy to provide the output necessary for the desired application, such as operating a self-contained wireless sensor network node. In the prior example, the EH circuit conditions collected small packets of energy to provide the required voltage-output and current output conditions to operate the temperature sensor and the wireless ZIGBEE transmitter.

2.3 The Power over Fiber Technology

A new type of technology appeared from the junction of the solar energy theory, the fiber optics and Energy Harvesting (EH). As we know, a fiber optic is a glass or plastic fiber that carries light along its length. Optical fibers are widely used in fiber-optic communications, which permits transmission over longer distances and at higher bandwidths than other forms of communications. Fibers are used instead of metal wires because signals travel along them with less loss, and they are also immune to electromagnetic interference. Light is kept in the core of the optical fiber by total internal reflection, and by that, new ideas came up, to feed some important parts of an optical fiber network that could not be reached by copper cables or other type of cables, due to electromagnetic interferences or hazardous places. This was how the Power over Fiber (PoF) idea began.

The PoF is a technology that is based on the light that travels through the fibers, that is collected, in this case harvested, by a photodiode (Pd), and then transformed, so it can be used to feed all the internal components of a node in a Passive Optical Network (PON). A PON is a network where there is no electricity at all, that's why the light that travels through the fiber needs to be harvested, to enable that the electrical components of the network could have some sort of energy source.

Photodiodes are a type of photodetectors and exist in different materials such as germanium (Ge), Silicon (Si) or Indium Gallium Arsenide (InGaAs) because each material has its own way to adapt itself to a different wave length. There are two types of photodetectors, PIN and APD.

The PIN photodiode is created adding an intrinsic region between the regions P and N. The intrinsic region has a high resistivity and therefore it's necessary low reverse polarization to cause the enlargement of the high field region (depletion region), which will present greater width compared with a simple pn junction.

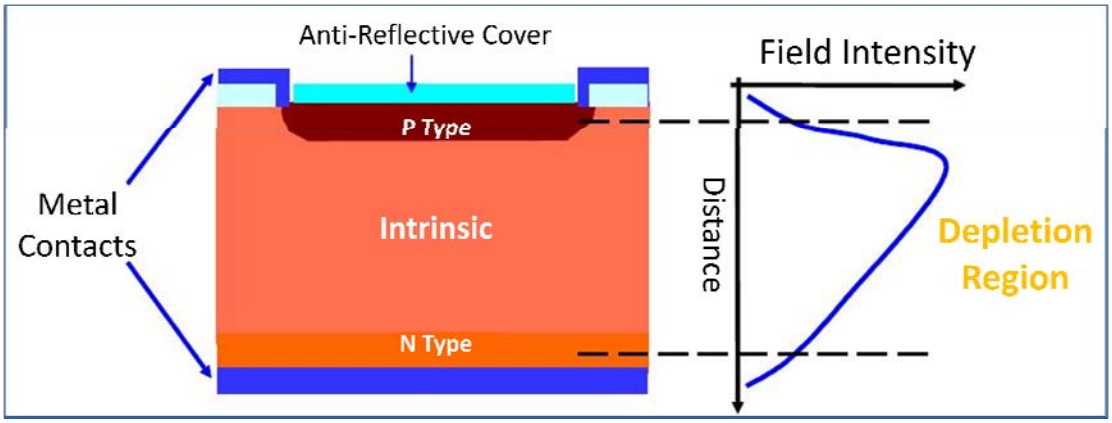

Figure 5 - PIN Internal Structure

Due to a bigger thickness of the depletion region, the PIN structure presents a smaller junction capacity (higher band width). The rise of the depletion region leads to a higher absorption of the major incident photons and consequent rise of the electron-gap pairs, being this a condition to a good photodetector response (21).

The resistance value of the PIN diode is determined only by the forward biased DC current. In switch and attenuator applications, the PIN diode should ideally control the RF signal level without introducing distortion which might change the shape of the RF signal. An important additional feature of the PIN diode is its ability to control large RF signals while using much smaller levels of dc excitation.

The performance of the PIN diode primarily depends on chip geometry and the nature of the semiconductor material in the finished diode, particularly in the Intrinsic region, see Figure 5, these characteristics enhance the ability to control RF signals with a minimum of distortion while requiring low dc supply (22).

As for the APD, the Avalanche Photodiode is a specialized PIN photodiode to operate with high reverse bias voltages. Large reverse voltages generate high electric fields at the P-N junction. Some of the electron hole pairs passing through or generated in this field gain sufficient energy to create additional electron hole pairs. If the newly created electron hole pairs acquire enough energy, they also create electron hole pairs. This is known as avalanche multiplication and is the mechanism by which APDs produce internal gain. The internal structure can be seen in Figure 6.

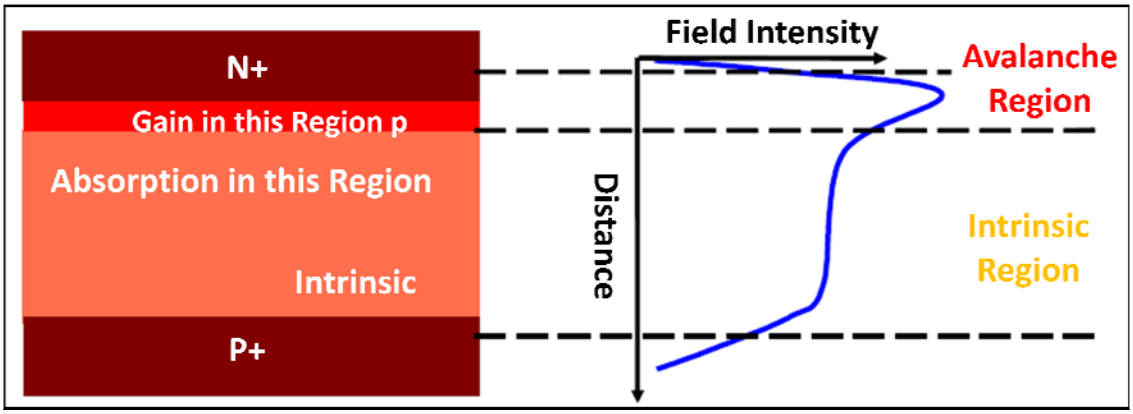

Figure 6 - APD Internal Structure

PIN regarding the APD, are not noisy, they are not so sensitive to temperature changes and polarization voltages and besides all that, and the main reason because it were chosen, they are cheaper.

Power over Fiber technology was chosen, among others, because Passive Optical Networks are already a reality, but, as all new technologies, it has its flaws and some improvements to do, being this work, one of those improvements. This work is not only applicable to PON, as there are other types of devices that may have this kind of voltage source.

The problem to resolve, as described in this document, is a creation of a DC-DC step-up converter where the input voltage is collected through a photodiode. Having a optical power of about 0dBm and being the photodiode efficiency around 40%, it collects the energy that is circulating in the fiber optic and transforms it to a voltage about 400 mV and a current of 1mA. Those 400 mV need to be raised up to about 5 volts to feed all the internal hardware in the remote node. The node already has its own storage system, and thus when no action is required by the internal hardware, the voltage harvested by the photodiode can be stored to be used later.

2.4 PON – Remote Nodes – The Available Solution

Passive optical networks (PONs) are becoming consistent alternatives to offer access solutions in a fiber-to-the-home (FTTH) environment. Flexibility, scalability, resiliency, higher user density and bandwidth, robustness and extended reach are some of the important features for the next generation PONs (NG-PONs), while maintaining simplicity to make the network economically practicable and accessible to normal users.

Scalable Advanced Ring-based passive Dense Access Network Architecture (SARDANA) is an attempt to demonstrate how to exploit NG-PON in a cost effective and reliable way, allowing migration from the current deployed Ethernet PON (E-PON) and Gigabit PON (G-PON). SARDANA network is able to reach more than 1000 users spread over 100km, with symmetric 100Mbit/s per user (11). This network consists on a hybrid wavelength division multiplexing (WDM) double ring and time division multiplexing (TDM) tree topology connected by means of a remote node (RN) which guarantees the scalability of the network. One major component of these networks is the remote nodes and his lack of powering (23), being also an important component in the re-configurability of the network, mainly its power converter, control and harvesting module.

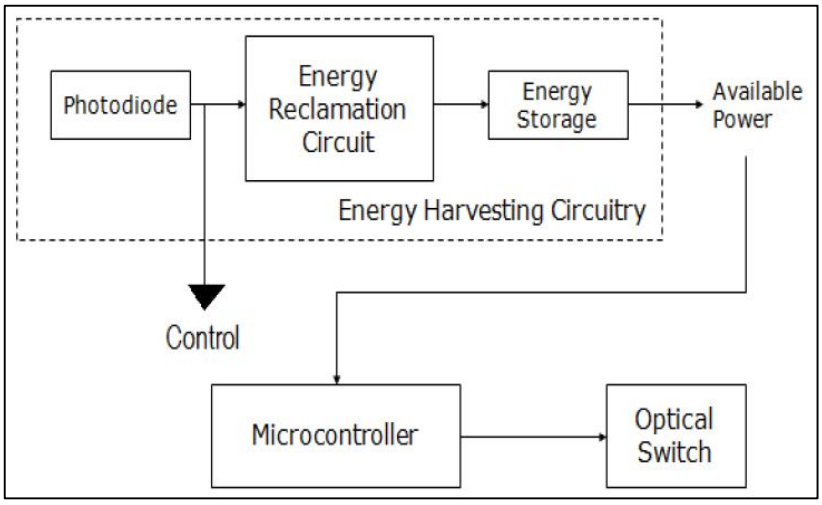

Figure 7 - Schematic of the Harvesting and Control Module

Figure 7 shows the block diagram of the equipment inside the module. An optical signal, composed only by light, is received by a photodiode present on the module where is a part of the optical to electric conversion. Part of this converted electrical signal is provided to a control unit by means of a Radio Frequency component. The mainly part of the

converted energy is supplied to an Energy Reclamation Unit to be stored and used to control the switches.

A. Baptista in his master thesis demonstrated, for this kind of power converter and harvesting modules that the efficiency is higher for input optical powers between -7 and 0dBm and the output electrical power is higher for higher input optical power, so, the best operation point of this conversion unit is for 0dBm (12). Experimental tests were made on these modules to demonstrate the possibility to control the unit with power as low as -25dBm, although, the minimum power for harvesting is much higher than that, what can be difficult to achieve if multiple modules are implemented in a very large network, as can be seen in the paper entitled "Remotely Reconfigurable Remote Node for Hybrid Ring-Tree Passive Optical Networks", by A. Baptista, M. Ferreira, A. Quinta, M. Lima and A. Teixeira (24).

A device with a similar methodology was investigated by H. Ramanitra, P. Chanclou, Z. Belfqih, M. Moignard, H. Le Bras and D. Schumacher (25), the Variable Optical Splitter (VOS) is an advanced component which can integrate access PON in the future. The active component with tunable coupling ratio can be activated using a remote powering technology via fiber-optic. This new technology avoids using a local power supply via a power line.

The VOS powering system is shown in Figure 8. The key element of this system is a pigtailed Power Converter Module (PCM) (26). The PCM converts optical power carried in the fiber into electrical power to activate the VOS. The output voltage and current depend on the optical power injected into the module. The maximal output voltage achieved by them was about 5*Volts* whereas the output current varies between 1 and 60*mA* for an injected light in the range of [+1, 23]*dBm*. As a power source, they used lasers implemented in the CO has a normal optical network. Using a wavelength multiplexer, the data (1.49μm) and the powering optical channels ($\lambda p1$, $\lambda p2$, $\lambda p3$) are carried by the same existing fiber. A demultiplexer, placed inside the base Distribution Frame (DF_b) extracts the wavelengths that

are then injected into the photovoltaic modules. PCMs are electrically linked to each 1x2 VOSs and there for, the active splitters can be remotely powered and controlled by varying the optical power emitted from the CO. This innovative powering system avoids using a local power supply or power lines, and still maintains the network completely passive and makes it reliable and flexible with a low cost.

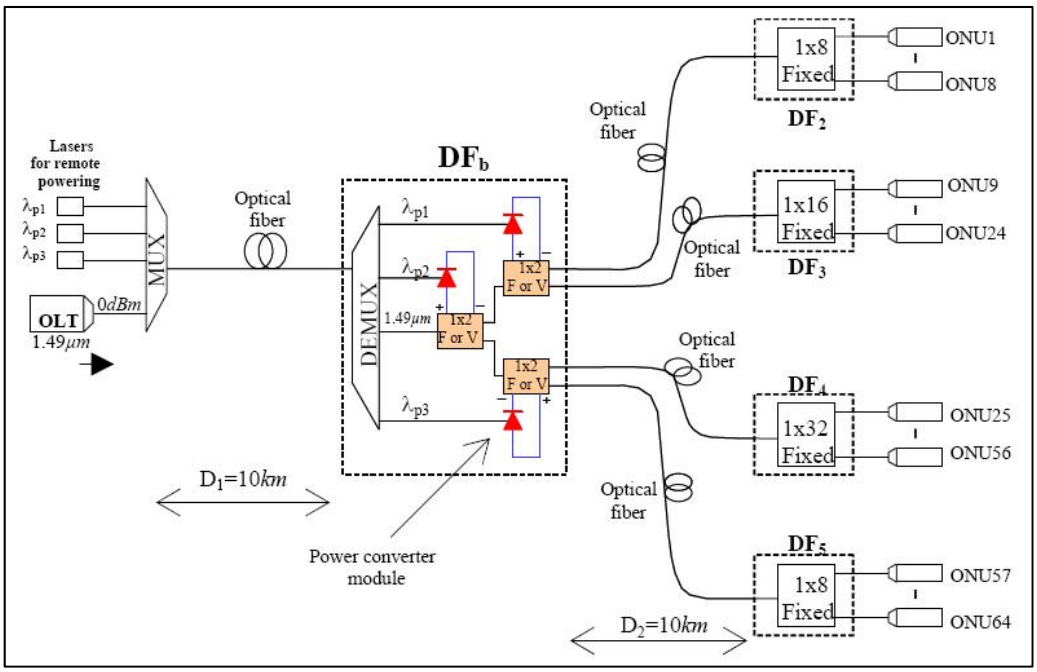

Figure 8 - Access PON architecture with VOS(25)

The 1x2 VOS needs a driving voltage of 435mV and a driving current of about 40mA. Variation of 1x2 VOS transmission versus optical power injected inside the photovoltaic module is shown in Figure 9. When there is no voltage applied to the VOS, data is transmitted in quasi full in the first output fiber. The transmissions *T01* and *T02* begin to be progressively reversed from 6*dBm* of powering light. The transmission completely switches on the second output at about 19*dBm*. The 50-50% coupling ratio is obtained for a PCM injected light of around 10.7*dBm*. Considering the Insertion losses of the wavelength Mux and Demux , let's say about 4*dB*, and the fiber attenuation, about 0.25*dB/km*, the powering system needs a maximal optical budget, from the Central Office (CO), of about 25*dBm* to remotely activate the VOS at a range of 10*km* (25).

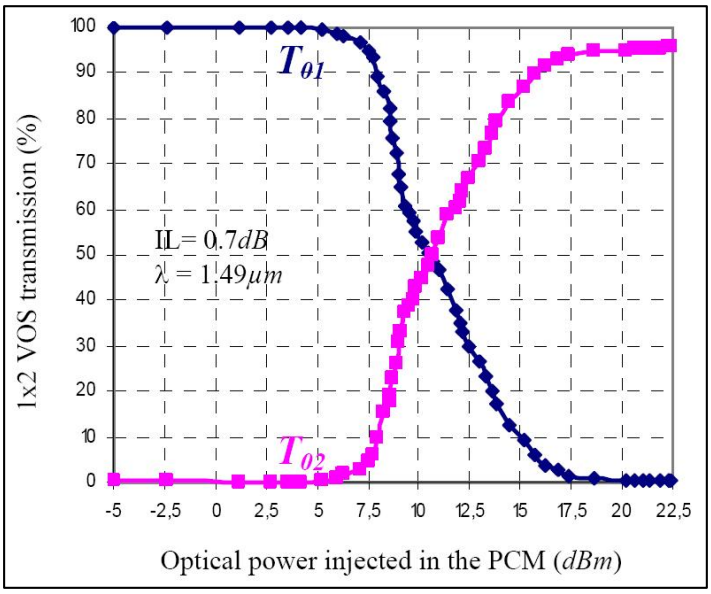

Figure 9 - Variation of 1x2 VOS transmission versus powering light

Being this the proposal for a remotely powered optical node an exhaustive search is required. Find technologies that can help to improve this concept or make something new that can be an improvement of this concept, for instance, the Harvesting module and the DC-DC converter, both important parts of the Energy Reclamation Circuit block in Figure 7. To start, an evaluation of the existing low voltages or ultra low voltages commercial sources and Harvesting modules must be carried on with the criteria of the problem in hands.

2.5 LV/ULV Commercial Sources and Harvesting Modules

Nowadays the commercial integrated circuits for low or ultra low voltages are very common. The only defect of those commercial circuits is that they have high startup voltages. For instance the LM2621, from National Semiconductor, it has a very good output voltage range, 1.24V to 14V, and a good switch current, but the minimum input voltage is

too high for an ultra low voltage DC-DC Step up Converter, the minimum input voltage is about 1,2V.

One commercial circuit that specific says that is an ultra low voltage device is S-882Z, a Charge Pump from Seiko Instruments. A Charge Pump is a kind of DC to DC converter that uses capacitors as energy storage elements to create either a higher or lower voltage power source. Charge pump circuits are capable of high efficiencies, sometimes as high as 90-95% while being electrically simple circuits. Returning to the S-882Z from Seiko, this device has a minimum input voltage of about 0,3 volts, but the main problem is that it consumes, in operating mode, about 0,5 milliamp, and that's 50% the 1 milliamp available. Other disadvantage is that it is only an external device of a DC-DC converter and, if the S-882Z alone consumes a lot of current, plug it series with a DC-DC converter, that by itself needs more power, it would consume more than the limit available.

In 2007, Advance Linear Devices launched their first energy harvesting Module, the EH300 Series. These modules were designed for low power intermittent duty and long storage time applications. Specific onboard functions include energy capture and accumulation, energy storage, power conditioning and energy management from various energy sources, such as solar cells, PZT piezoelectric ceramic composite elements, inductive elements and micro thermal-electric generators. EH300 Series Modules can easily adapt to a variety and wide range of voltage and power inputs and outputs. Energy can be collected from many types of secondary or waste by product environmental sources, such as thermal, mechanical, chemical, solar, biological and human body sources (27).

There are also other commercial circuits that could serve the general purpose of this work such as the L6920 from ST Microelectronics (ST), and the TPS61200 from Texas Instruments (TI). Both have a very low input voltage start, and good output Voltage levels, as it is stated in each one datasheet.

2.5.1 The EH300 Harvesting Module from ALD

It is stated in the EH300/EH301 Series datasheet's that EH Modules can accept energy from many types of electrical energy sources and store this energy to power conventional 3.3V and 5.0V electrical circuits and systems such as wireless sensor networks (WSN) any other low or ultra low power electronics. EH300/EH301 Series Modules are completely self powered and always in the active mode. They can function with instantaneous input voltages ranging from 0.0V to +/-500V AC or DC, and input currents from 200nA to 400 mA. Harvested energy can be collected from sources that produce electrical energy in either a steady or an intermittent and irregular manner with varying source impedances. EH300/EH301 Series Modules condition the stored energy to provide power at output voltage and current levels that are within the limits of a particular electronic system power supply specification(27)(28).

2.5.2 The L6920 Integrated Circuit by ST Microelectronics

The L6920 is a high efficiency step-up controller requiring only three external components to accomplish the conversion from the battery voltage to the selected output voltage. The startup is guaranteed at 1V and the device is operating down to 0.6V. Internal synchronous rectifier is implemented with a 120mΩ P-channel MOSFET and, in order to improve the efficiency, a variable frequency control is implemented (29).

2.5.3 The TPS61200 Integrated Circuit by Texas Instruments

The TPS61200 device provide a power supply solution for products powered by either a single-cell, two-cell, or three-cell alkaline, NiCd or NiMH, or one-cell Li-Ion or Li-polymer battery. It is also used in fuel cell or solar cell powered devices where the capability of handling low input voltages is essential. Possible output currents are depending on the input to output voltage ratio. The devices provides output currents up to 600 mA at a 5-V output while using a single-cell Li-Ion or Li-Polymer battery, and discharge it down to 2.5 V. The boost converter is based on a fixed frequency, pulse-width-modulation (PWM) controller using synchronous rectification to obtain maximum efficiency. At low load currents, the converter enters the Power Save mode to maintain a high efficiency over a wide load current range. The Power Save mode can be disabled, forcing the converter to operate at a fixed switching frequency. The maximum average input current is limited to a value of 1500 mA. The output voltage can be programmed by an external resistor divider, or is fixed internally on the chip. The converter can be disabled to minimize battery drain. During shutdown, the load is completely disconnected from the battery (30).

2.6 Evaluation of the commercial Circuits

For a proper evaluation of both Integrated Circuits, the datasheets suggest a test circuit for each one. Those circuits were built on a Breadboard for test on laboratory being the primary objective, test the veracity of the data on the respective datasheets, and how both circuits would respond in real time tests.

The harvesting module is already an assembled circuit, so the only thing to do for testing is to plug it in to a variable voltage source and verify the veracity of the datasheet values.

2.6.1 ST's L6920

The circuit present on Figure 10 was built on a breadboard with the aim of testing the datasheet values, and if it would answer to our specific problem.

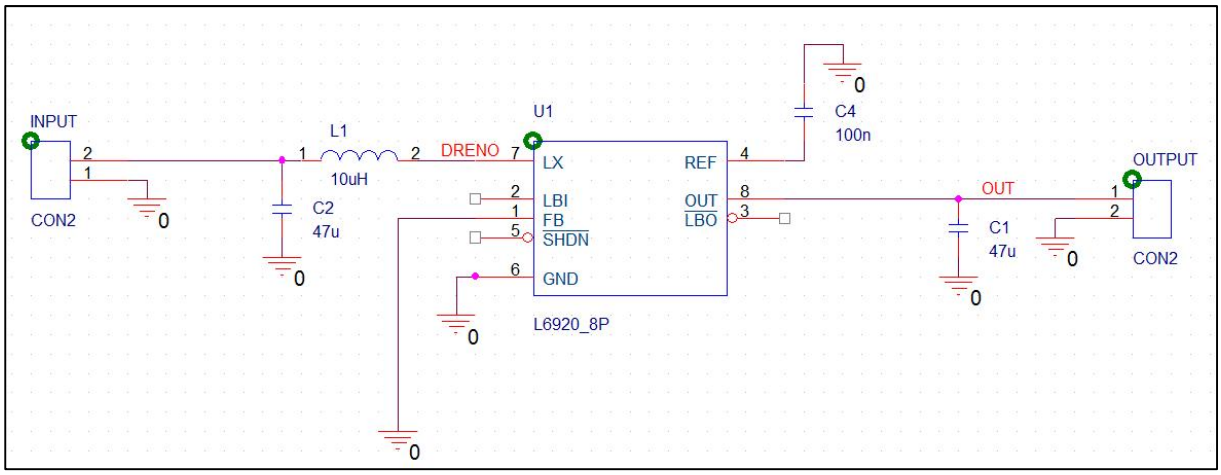

Figure 10 - L6920 Breadboard Test Circuit

The first thing that came up was the startup voltage, the 1 V stated in the datasheet does verify, it started to work with an input voltage of about 0.9V, the datasheet also states that it remains in operation until de input voltage drops below 600 mV, and that was confirmed too.

The current consumption of the L6920 described by the datasheet is also correct. The L6920 has a Quiescent Current of about 9uA to 15 uA, and a shutdown current of 0,1uA to 1 uA. As for the current consumption for a 10KΩ it was about 7mA. These current values are high but acceptable if we take into consideration that they are within the same order of magnitude as the 1mA.

Resuming, this integrated circuit besides having a high start voltage value and a acceptable current consumption and it may be useful for step-up an input voltage of about 1.2V to the required 5 V without consuming much more current.

2.6.2 T.I.'s TPS61200

Following the previous point, the test circuit present in the datasheet circuit was built like the one that is present on Figure 11. It was built on a breadboard with the aim of testing the datasheet values, and if it would answer to our specific problem.

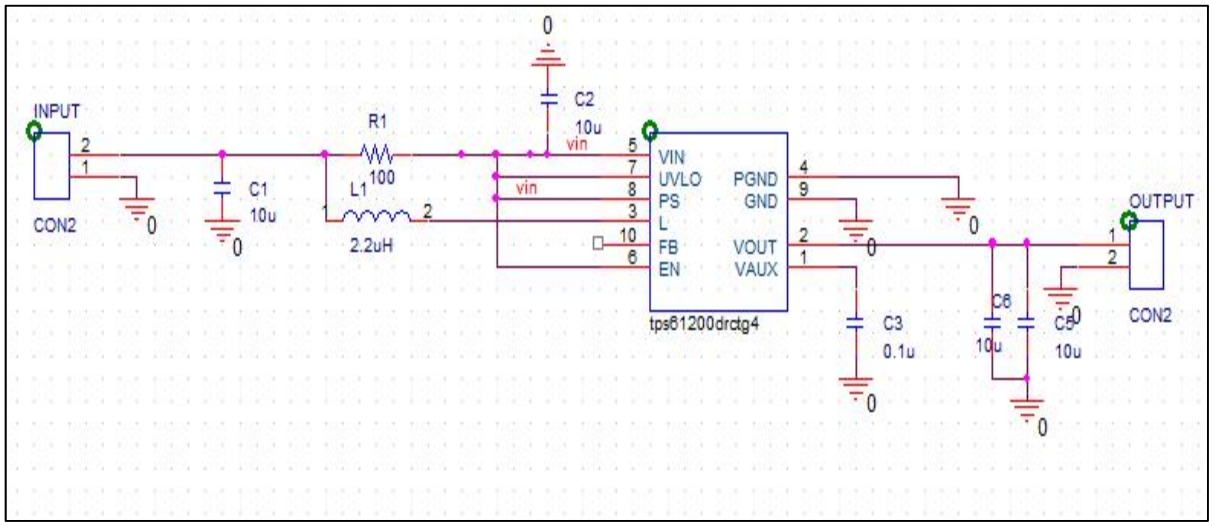

Figure 11 – Breadboard TPS61200 Test Circuit

The startup input voltage is about 0,95V, and it almost achieves the necessary 5 V more exactly the output is 4,5 V.

The current consumption is, at the startup, about 56mA, and at the maximum output voltage,6,6V, also about 56mA, with no load. With a 10KΩ load the startup voltage maintains equal but the current consumption rises to 71,5 mA. From this work point of view it will drain too much current when loaded, taking into account that it has only 1 mA available to consumption, it is not an alternative to consider!

2.6.3 ALD's Harvesting Module – EH301

This module, Figure 12, promised to be the most straightforward strategy. According to the datasheet[i]. It could be used with a minimum operational input of 0.0V@1nA. and would implement directly almost all the prerequisites that were imposed. The exception would be the normal behavior of the module, which by default is configured to discharge whenever the maximum voltage was achieved. This way, extra control electronics would still be necessary.

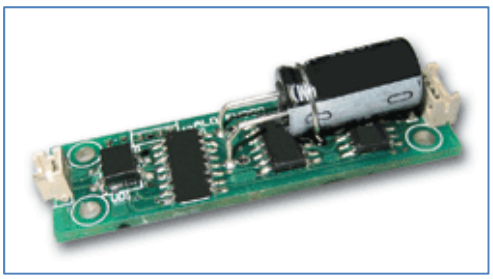

Figure 12 - Energy Harvesting Module

This proved to be an unsuccessful strategy, up to now. After the arrival of the device, initial tests proved that it did not work according to the datasheet description. Even with a 1.5 V battery connected directly, it still would not work. The main reason for that was the very incomplete and misleading datasheet description of the module which stated that it could "begin operating from 0.0 V". Apparently, the energy source does require a minimum of 6 V and 300 nA in order to charge up the EH301 module, being this information provided by ALD. For lower input voltages from the energy source, a low voltage to higher voltage converter, such as an AC to AC step-up transformer, or a DC to DC up converter, may be needed at the input as an interface between the energy source and the EH301 module. If this had not been omitted in the datasheet, this module would not have been considered for the intended purposes.

Besides what was indicated above, the output voltage cycles between a high output voltage and a low output voltage of V_L=3.1 V and V_H=5.2 V. These voltage levels are intended to correspond to a minimum and a maximum operating voltage of a load circuit, and should operate such a load circuit directly if the load circuit has been designed for battery operation. Also, for the specific case where its use is intended, external control circuitry is needed to control when the energy is to be released through an alternative path or when to actually load the intended charge. To prevent overcharging, the energy cannot be released

through the load path, because this would activate the switch. One even worst consequence of that procedure would be the waste of energy that took a long time to harvest. To avoid that, further circuitry would have to be included again.

2.6.4 Conclusions

The test circuits suggested by both datasheets were built on a breadboard. Each one was tested with a variable lab voltage source too find the startup point for each integrated circuit. The harvesting Module was also tested in laboratory but directly connected to a variable power supply and with a 1,5V battery.

For the L6920, from ST, the startup voltage was a bit high for this work purposes. The 1V at the input is a value too high, the optimal startup voltage should be about 400 mV, or less.

The TPS61200 was put aside due to its current consumption when loaded. The 71,5mA, when loaded is a value too high for this work. The maximum current that it could consume is about 1 mA or less, in a very optimistic view.

As for the Harvesting Module it was tested in lab with the appropriate power supply, and also was done a test with a 1.5 V battery, that returned unsuccessfully. The startup voltage values have also proved to be incorrect, and there for it is a circuit not to have in consideration.

The best characteristic of the TPS61200 is the startup voltage, the 0,95V should be a good power stage for this work, but the high current consumption is the worst characteristic, and decisive about setting aside this integrated circuit.

Concerning the L6920, the best characteristic is the low current consumption. The Startup voltage is a bit high but, nevertheless, is low enough for giving it a try to make it work as a power stage in this work.

The Harvesting Module its very well build and it considers every aspect related to energy harvesting and storing. It is always powered on, and does not have a standby mode, nevertheless it needs very low current to maintain it operation.

Resuming, the TI's integrated circuit was put aside due to the high current consumption, but the ST's integrated circuit is still a possibility on the table due to its low current consumption although it does have a startup voltage a bit high for the requirements. For the harvesting module, the wrong values described in the datasheet for the startup voltage were the negative points for this module, and the main factor to have been set aside.

Chapter 3: Enabling Power over Fiber

3.1 The Problem

A low-level power transmission system based on laser light conducted through fiber optics promises to reduce the risk of interfacing to physical communications channels on the electrical grid. The system available now and referred to as power over fiber (PoF), provides practically infinite voltage isolation capability, for instance, between a central office in a telecom network and a high-voltage transformer substation, as it can be seen in Figure 13. This isolating capacity increases the protection from hazards associated with ground-potential rise (GPR), which is common to high-voltage zones such as those surrounding power transmission equipment.

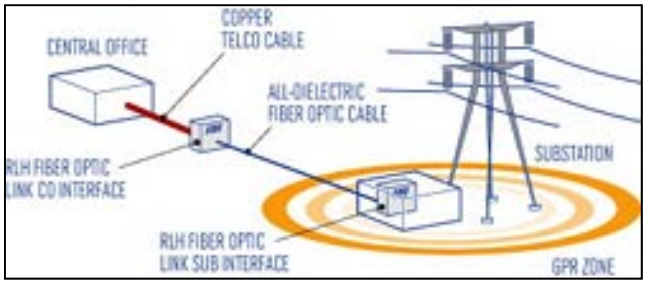

Figure 13 - PoF technology provides an option for terminating telecommunications copper lines to a modem outside the GPR zone surrounding a substation

Utilities industries may lease communication lanes on their infrastructures to communications providers, as well as for their own system-management functions, such as Supervisory Control and Data Acquisition (SCADA). It is often necessary to interface such

grid-based networks with conventional telecom networks. In cases where conventional ac power is unavailable, and options such as solar or wind power are not practical, this could mean running copper data lines directly to substation equipment. However, such installations are particularly prone to GPR hazards.

To preclude these hazards, the PoF system enables the copper-based data link from the telecom office to terminate into a remote fiber-optic modem. This modem then receives power (and sends and receives data) at a safe distance from the substation via optical fibers (see Figure 14). The all-dielectric nature of these optical fibers provides an electrical isolation across their entire length (unlike galvanic isolation, which is restricted to the insulation barriers within a transformer).

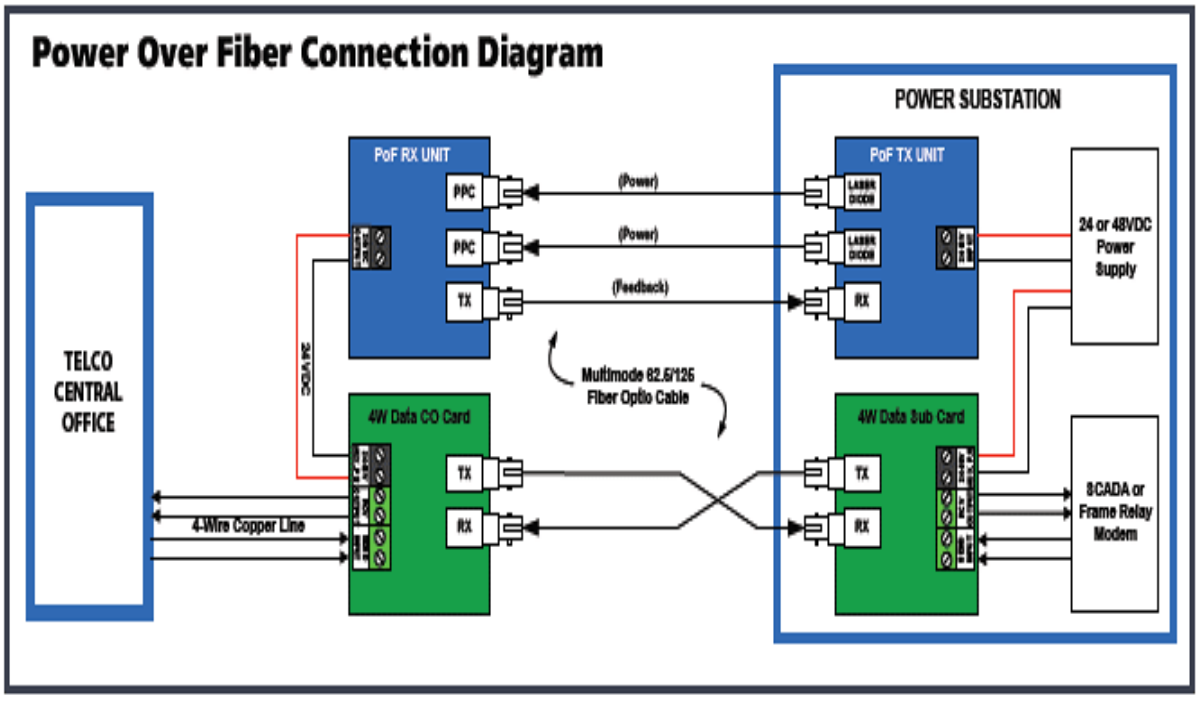

Figure 14 - PoF Connection Diagram

The basic PoF system consists of the transmitter (Tx) unit, located at the substation, and the receiver (Rx) unit, located at the remote fiber-copper interface. The two units are linked by three optical fibers. Two fibers transfer the power, with each fiber forming a single power channel for each of the two continuous-wave 830-nm laser diodes in the Tx unit. The

third fiber transfers a power-integrity feedback signal from a conventional LED in the Rx unit to a conventional optical receiver in the Tx unit.

The PoF's energy-transfer efficiency is low because the technology is new, and its main purpose is safety, not performance. The lasers in the Tx unit consume about 48 W in order to deliver about 720mW to the Rx unit. While power losses increase with fiber length, useful power is still transmitted at the maximum recommended fiber length of about 450 meters.

It's also stated that the lasers have a narrow operating temperature range that requires both active heating and cooling systems onboard the Tx unit. Therefore, the ambient system operating temperature for the Tx unit is from 0°C to 35°C, what requires more energy too be consumed too cool down, or in some other cases warm up, the Tx unit (31)

This document focuses a technology based on PoF. It is a technology that harvests on an optical fiber enough power to feed a remote node, or as been stated above, a modem, while it receives and transmits data, in a passive optical network.

The harvesting method consists on a photodiode that collects from the fiber about 400 mV @ 1 mA. Meanwhile a DC-DC method is required to step-up that voltage to a higher one that can power up the Programmable Interrupt Controller (PIC) and Optical Switches present in the remote node.

Those 400 mV at the input represent an obstacle, but the real problem is the current. The 400mv are a very low voltage and to allow its utilization, some special components must be used, such as low threshold MOSFETs, with low negative or even zero threshold voltage, or germanium transistors known by their high gain and low bias current, and all these components need current to work.

The 400 mV can be raised to a more useful value, but current must be consumed, being that the most critical problem. To build an efficient boost converter, to raise the voltage, an inductor, or more, needs to be placed on the base circuit and that means a raise on current consumption which increases the criticalness of the problem.

The main objective of this work is to raise the 400 mV, or lower, to a useful level that can be used to power up some external DC-DC circuit or, if possible, raise it to the necessary voltage, but without consuming more than the available current.

Being this the main goal of this work, the adopted solution is explained, step-by-step, in the following chapter.

3.2 The Solution

To begin, the block diagram present in the Figure 15 will be explained, as it globally represents the first idea to solve the problem. The idea refers to an ultra low power oscillator, made with some special EPAD MOSFETs from ALD (31), and a simple Boost Converter, named Pre-Boost Converter, to boost the input voltage up to power up a secondary stage. This is composed by a delay block that is necessary to allow the pre-boost to gain the necessary voltage to power a second oscillator, composed by a Schmitt Trigger that will produce a square wave with enough amplitude to switch the power MOSFET in the Power Boost Converter.

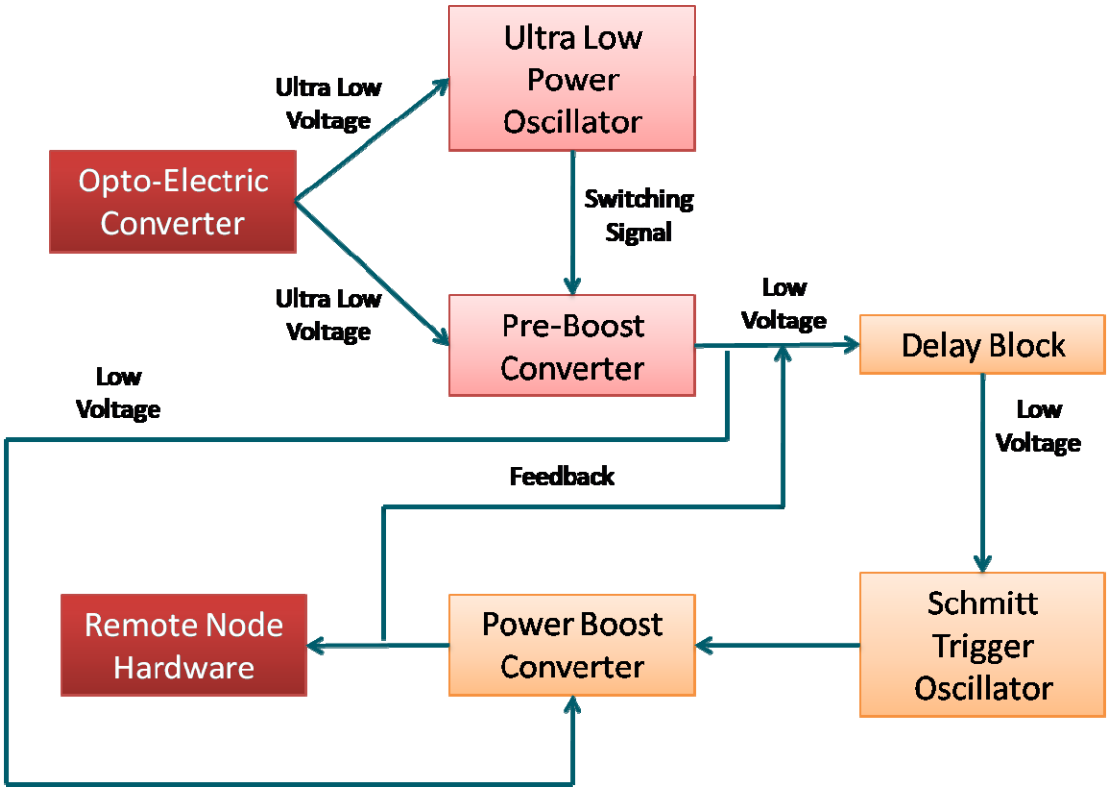

Figure 15 - Block Diagram

This solution resorted to an oscillator that could work at high frequency conjunction with an ultra low voltage source. The oscillator circuit was easy to figure out as it was chosen the astable multivibrator due to the fact that it does not have any stable state, which means that is always oscillating between one state and the other. The tricky part was to make it work with the low or ultra low power available. A solution came up with the new EPAD MOSFETs from ALD, in particular the ALD110800 that has zero threshold voltage, which means is closed for gate voltages above 0.0V, and it is open below that value. Among these EPAD MOSFET's, this zero threshold voltage is called an Enhancement Mode MOSFET, but there are others with interest that are called Depletion Mode MOSFETs, in particular the ALD114804, that has a negative threshold voltage, precisely -0.4V, and it proved to be a good attack switch for the Pre-Boost Converter.

The Pre-Boost Converter, as the Power Boost Converter, is as simple as it could be. It is a boost converter that makes the output voltage higher than the input.

After the pre-Boost Converter, the next block is composed by two Schmitt Triggers from Texas Instruments and their main function is to create a bigger attack signal to the final block. The first stage, composed by a normal Schmitt Trigger, is only to delay the start up of the next Schmitt Trigger, being this an inverter Schmitt Trigger which with some external components can be used as an oscillator producing an attack signal with amplitude equal to the voltage of the pre-Boost Converter. Before the resulting signal can attack the Power MOSFET it also has a pull up resistor and a capacitor to increase the signal offset and, after this, it will attack the power MOSFET on the final block.

The final block is another boost converter but now optimized to a higher frequency and with a power MOSFET with a low threshold voltage.

For the Bootstrap technique, the main idea was to store a sufficient energy amount in the first boost capacitive load and increasing the supply voltage in the Schmitt Triggers block. This way the last switching signal excursion will increase and attack the switch in the final boost converter with even more amplitude, increasing the output voltage of the Boost Converter and, there for, the output voltage, and in case of failure of the input voltage, it can be by itself for a determined period of time.

Chapter 4: Ultra Low Voltage Source – EPAD MOSFETs

4.1 The Astable Oscillator

Getting any electronic circuit to operate below one volt is a real challenge. Typical silicon bipolar transistors don't work below 0.7 volts. Some old germanium transistors do work down at low voltages but those are hard to find and are usually offered only in large packages. Many energy harvesting systems generate low voltages. Fuel cells, vibration transducers, thermoelectric devices, RF detectors and photovoltaic cells will typically produce low voltages. For instance, a single solar cell will only produce 0.5 volts and this is well below any practical voltage and, for this reason, some type of DC to DC converter would be needed to boost the voltage to some useful level.

At the heart of any DC to DC converter is an oscillator. If an oscillator does not run with the available voltage, it would not be possible to boost up that voltage. After some research and some thought about the various ways to design a low voltage oscillator, it was decided to try some new zero threshold voltage n-channel FETs from Advanced Linear Devices (ALD), the ALD 110800(32). These devices are two pairs of transistors in a 16 pin package, each pair with a common source connection. By carefully picking the component values, the circuit operates from about 0.2 V to over 0.6 V.

The circuit on Figure 16 is an astable multivibrator. The multivibrator is an electronic circuit used to implement a variety of simple two-state systems such as oscillators, timers and flip-flops. It is characterized by two amplifying devices, in this case two MOSFETs, cross-coupled by resistors and capacitors. The most common form is the astable or oscillating type, which generates a square wave and, in this case, with a frequency of about 3 KHz. A

higher frequency is possible by changing the two external capacitors to smaller values, but the wave signal becomes sinusoidal and with very low signal excursion, for instance, for an input voltage of 300 mV, the signal only reaches about 100 mV.

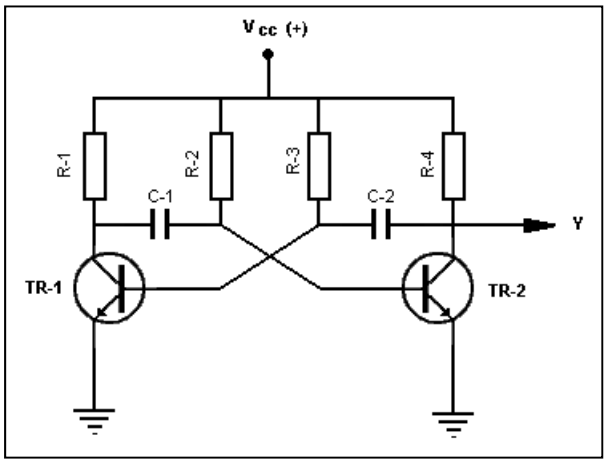

Figure 16 - Astable Multivibrator with Bipolar Transistors

EPAD MOSFETs

The bases of the oscillator are two enhancement mode EPAD MOSFETs, with zero threshold voltage as been stated before. These unique devices are MOSFET matched-pair arrays with electrically-programmable thresholds (EPADs). EPAD is an analog technology innovation by ALD in which a unique CMOS MOSFET's threshold voltage and on-resistance characteristics can be electrically programmed to a precise level. Once programmed, the set parameters are indefinitely stored within the device even after power is removed. This technology employs a floating gate structure which can be precision trimmed to produce tightly controlled electrical characteristics in the transistor (33; 34)

- ***Enhancement Mode MOSFETs – ALD110800***

This ALD model was also built for minimum offset voltage and differential thermal response and it was designed for switching and amplifying applications where low input bias

current, low input capacitance and fast switching speed are desired. For the ALD110800 the $V_{gs(th)}$ is set at +0.0V, , which classify it as an enhancement mode device. When the gate is set at 0.0 V, the drain current is equal to +1 uA @ V_{ds} = 1 V, which allows a class of circuits with output voltage level biased at or near input voltage without voltage level shift. This device also exhibit well controlled turn-off and sub-threshold characteristics as standard enhancement mode MOSFETs.

- ***Depletion Mode MOSFETs – ALD114804***

These models are excellent functional replacements for normally-closed relay applications, as they are normally on (conducting) without any power applied, but could be turned off or modulated when system power supply is turned on. These MOSFETS have the unique characteristics of, when the gate is connected to GND, operating in the resistance mode for low drain voltage levels and in the current source mode for higher voltage levels and providing a constant drain current.

ALD114804 is a depletion mode MOSFETS and was built for minimum offset voltage and differential thermal response. It is suitable for switching and amplifying applications in single supply (0.4V to + 5V) or dual supply (+/-0.4V to +/-5V) systems where low input bias current, low input capacitance and fast switching speed are desired. This device exhibits well controlled turn-off and sub-threshold characteristics and therefore can be used in designs that depend on sub-threshold characteristics.

- ***Typical Features***

- Depletion mode (normally ON);

- Precision Gate Threshold Voltages: -0.4V +/- 0.02V;
- Nominal RDS(ON) @VGS=0.0V of 5.4KΩ;
- Matched MOSFET to MOSFET characteristics;
- Tight lot to lot parametric control;
- Low input capacitance;
- VGS(th) match (VOS) - 10mV;
- High input impedance - 10^{12} typical;
- Positive, zero, and negative VGS(th) temperature coefficient;
- DC current gain >10^{8};
- Low input and output leakage currents;

- ***Examples Applications***

- Functional replacement of Form B (NC) relays;
- Precision threshold voltage mode;
- Ultra low power (nanowatt) analog and digital circuits;
- Ultra low operating voltage (<0.2V) analog and digital circuits;
- Sub-threshold biased and operated circuits;
- Zero power fail safe circuits in alarm systems;
- Backup battery circuits;
- Power failure and fail safe detector;

- Source followers and high impedance buffers;
- Precision current mirrors and current sources;
- Capacitive probes and sensor interfaces;
- Charge detectors and charge integrators;
- Differential amplifier input stage;
- High side switches;
- Peak detectors and level shifters;
- Sample and Hold;
- Current multipliers;
- Discrete analog switches and multiplexers;
- Discrete voltage comparators.

- Validation of the Simulation Models

To understand in more detail these ALD MOSFETs, a simulation model was requested to ALD, since it was not available online. To test the models ALD100800 and ALD114804 in specific, a simple simulation circuit was built on Orcad Capture thus allowing to confront and analyze the values in the datasheets.

ALD110800

The model was tested with a common source configuration, as it can be seen in Figure 17, with the intent of measuring the $V_{GS(th)}$:

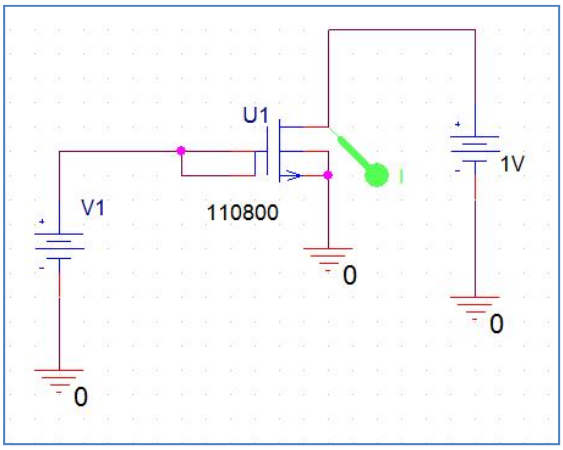

Figure 17 - ALD110800 Simulation Circuit - Common Source

It was simulated a DC sweep, between -0.25V to 0.25, on the ALD110800's gate, V1, and a drain tension equal to 1V as described in the manual.

The parameters shown on the datasheet for the ALD110800 are:

Parameter	Symbol	Min.	Typ.	Max.	Test Conditions
Gate Threshold Voltage	VGS(th)	-0.01	0.00	0.01	VDS=1V IDS=-1uA

Table 1 - ALD110800 Datasheet Values

The simulation resulted is shown in Figure 18.

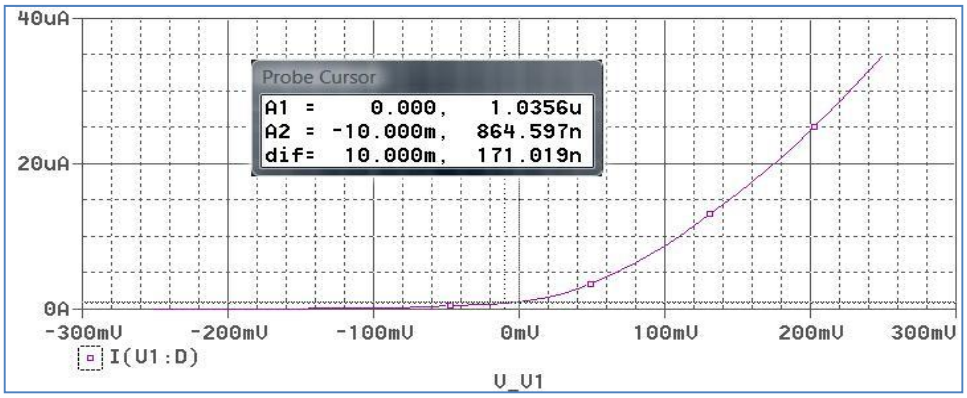

Figure 18 – ALD110800's Simulation Results

The results were within the expectations, as described in the ALD110800 datasheet.

In near zero $V_{gs(th)}$, shown in Figure 18 as the cursor A1, there is a Drain current of 1uA. The cursor A2 shows the minimum value that is mentioned in the datasheet, in this case, for a V_{gs}=-0.01V we already have a I_{ds}=864,6 uA approximately.

ALD114804

To test this depletion mode MOSFET model, the common source circuit was used again in the simulator.

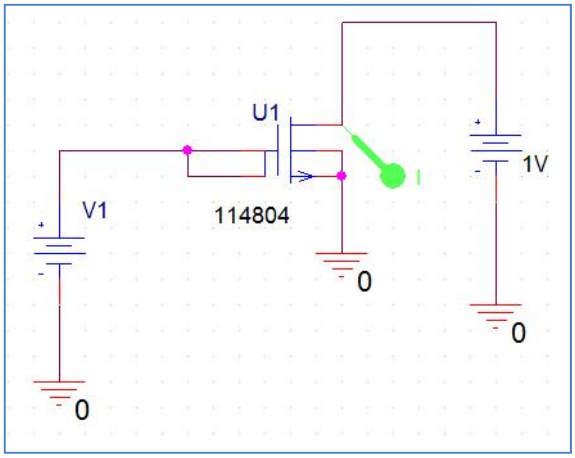

Figure 19 - ALD114804 Simulation Circuit - Common Source

For this specific model the datasheet values are those presented in the table below.

Parameter	Symbol	Min.	Typ.	Max.	Test Conditions
Gate Threshold Voltage	VGS(th)	-0.42	-0.4	-0.38	VDS=1V IDS=-1uA

Table 2 - ALD114804 Datasheet Values

The gate's tension was set between -0.6V and –0.2V, so the -0.4 threshold voltage could be tested.

As it can be observed in Figure 20, by the cursor A1, the V_{gs}=-0.4 does not correspond to the 1uA as described in the datasheet, instead it gives an Ids equal to 3.13uA. We can obtain the mentioned I_{ds}=1uA near the V_{gs}=-0.44V, which is a little bit off the values described in the datasheet.

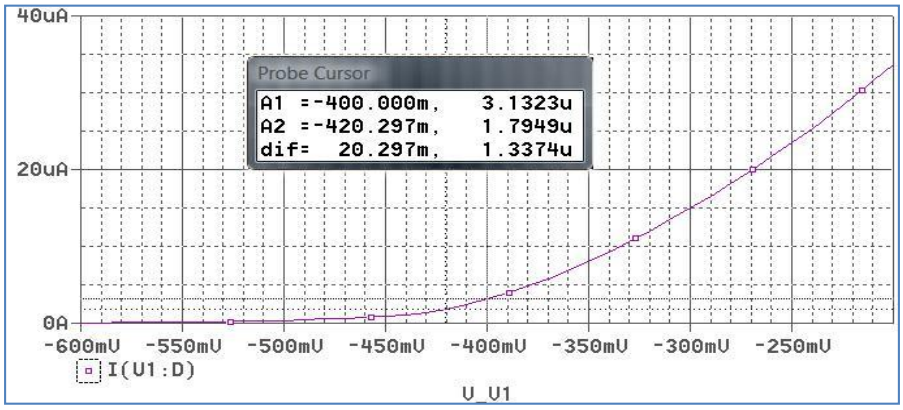

Figure 20 - ALD114804 - Vgs(th)=-0.4V

The minimum value, represented by the cursor A2, show us an Ids equal to 1.79uA, a little bit more that the 1uA expected.

- ***Conclusions***

All the simulations returned positive results compared with the ones contained in the datasheets of the respective components.

Regarding the models ALD110800 and ALD110802, the typical values where achieved. This way we can assume that that the Orcad's Model provided by Advanced Linear Devices is working in perfect conditions.

Although the ALD114804 model returned an output a little bit of the range value, this was not considered an important factor, because the MOSFET works inside the provided range, although conducting a little more current than the 1uA described in the datasheet.

As a final conclusion to this Chapter, all the models provided by ALD are able to be used in a more complex simulation.

4.1.1 The Oscillator Circuit – Theory

By carefully picking the component values, the circuit operates from about 0.2 V to over 0.6 V. The circuit described in Figure 21 is the astable multivibrator with EPAD MOSFETs. It is characterized by two amplifying devices, in this case two MOSFETs, cross-coupled by resistors and capacitors.

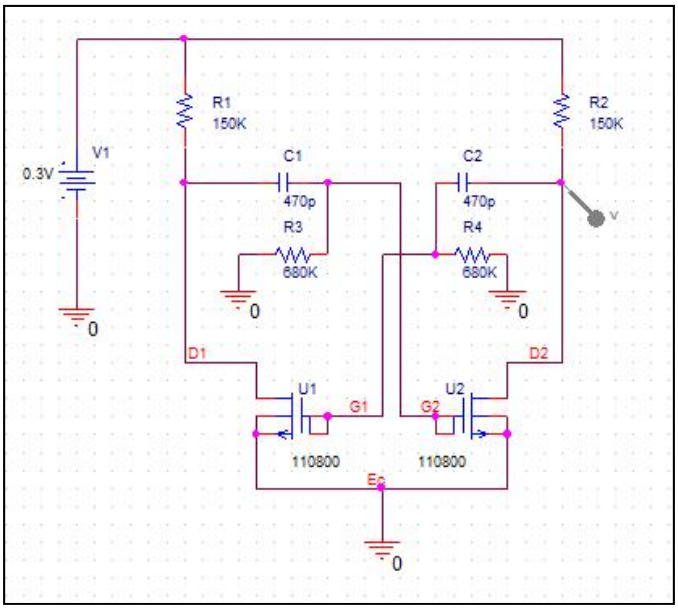

Figure 21 - Astable Oscillator - Base Circuit

It was verified that, with this configuration, the circuit did not work due to the lack of enough charge on the C1 capacitor that could not make the circuit to startup, a few changes were made. The C1 capacitor was charged and some capacitive charges, C3 and C4, were put and the resistors and capacitors values of each side of the oscillator were adapted to maintain the circuit balance.

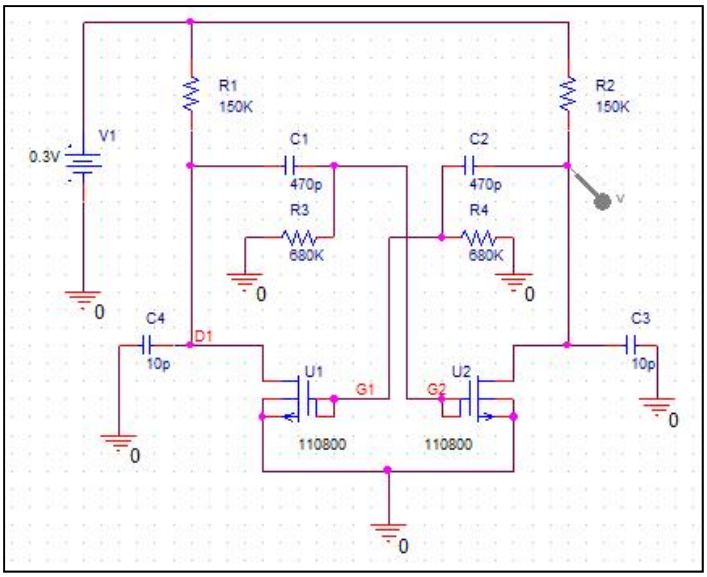

Figure 22 - Astable Oscillator - Final Circuit

Theoretically the oscillation frequency of this kind of oscillator should be given by:

$$i = \left(\frac{V}{R}\right)e^{-\left(\frac{t}{CR}\right)} \qquad (4.1.1.1)$$

In which *i(*A*)* is the electric current which changes in the time, *V* is the applied voltage, in this case 0.3 V, *R* is the resistance value in Ω, *t(*s*)* is the elapsed time after the charge beginning and the *CR* is the capacitive time constant (*CxR*).

The change of the voltage which is applied to the both edges of the resistor (R) is given by the following formula:

$$iR = Ve^{-\left(\frac{t}{CR}\right)} \qquad (4.1.1.2)$$

The moment, when this value becomes equal to the V_T, becomes the reversing time of the inverter.

$$V_T = Ve^{-\left(\frac{t}{CR}\right)} \qquad (4.1.1.3)$$

The reversing time (t), is given by the following formula.

$$t = -CR.\ln\left(\frac{Vt}{V}\right) \qquad (4.1.1.4)$$

The result is one half of the total period, the circuit configured with a 50% duty cycle of the period is T=2x*t*, and the frequency the inverse of the period. The frequency of the oscillator is then:

$$F = \frac{1}{T} = \frac{1}{2 \times t} = \frac{1}{2 \times \left(-CR.\ln\left(\frac{Vt}{V}\right)\right)} \approx 2085Hz \qquad (4.1.1.5)$$

Because the threshold voltage (V_T) depends on the I_d, it is sometimes different from the calculation result. When the value of the combination of C1 and R1, and the value of the combination of C2 and R2 are different, the time (T_H) of the high level condition and the time (T_L) of the low level condition are different. The condition with the time of the high level and the same time of the low level is called 50% of the duties. The frequency can also be changed and for that it is only necessary to act over the resistors and capacitors values.

Figure 23 shows the exactly output of the oscillator on the gray probe, Figure 22, an oscillation with almost 260 mV and a frequency of about 1.4 KHz.

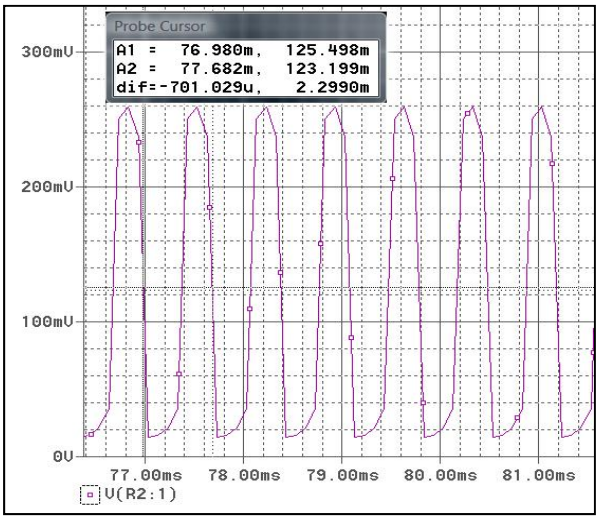

Figure 23 - Output Oscillation

The main reason explaining why the period does not suit the computation results includes the following.

- Discharging of the capacitor:

When the discharge of the capacitor is not done, the time when it reaches the threshold voltage becomes short.

- Threshold voltage(V_T)

It depends on the kind of the IC. The lower this voltage is, the longer the period becomes.

- Mathematical Errors in the Simulation Models or with the Simulator:

The models are not completely flawless and there may be some errors that the developers may have neglected, and there are also the simulator bugs or errors that also can contribute to some wrong results.

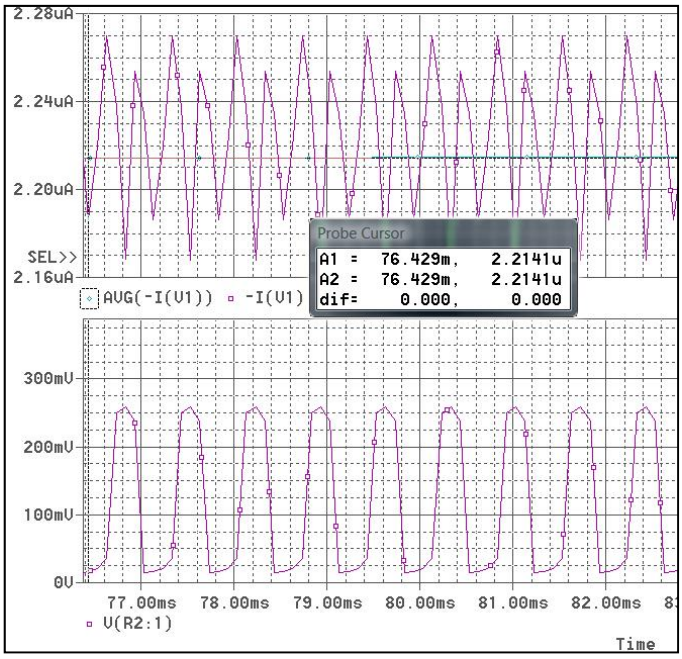

Figure 24 - Oscillator Output and Current Consumption

To observe the current consumption a probe was placed in order to measure the Source, V1, current. It consumes about 2.21 uA, as it can be seen on Figure 24, which is a very low value compared to some commercial oscillators and those commercial circuits also do not work with voltages as low For example, the 555 oscillator works with 5V and in astable mode it consumes about 3 mA (35). Another example is the integrated circuit from Texas Instruments, the 74AUC, that theoretically works with voltages down to 0.5V and it has a current consumption of about 10uA (36). It consumes low current but the feeding voltage makes its use limited.

4.1.2 The Oscillator Circuit – Laboratory Tests

To test the real capabilities of the oscillator and, therefore, the EPAD MOSFETs, a printed circuit board (PCB) was done. The Figure 25 shows the final board that will be tested in the laboratory.

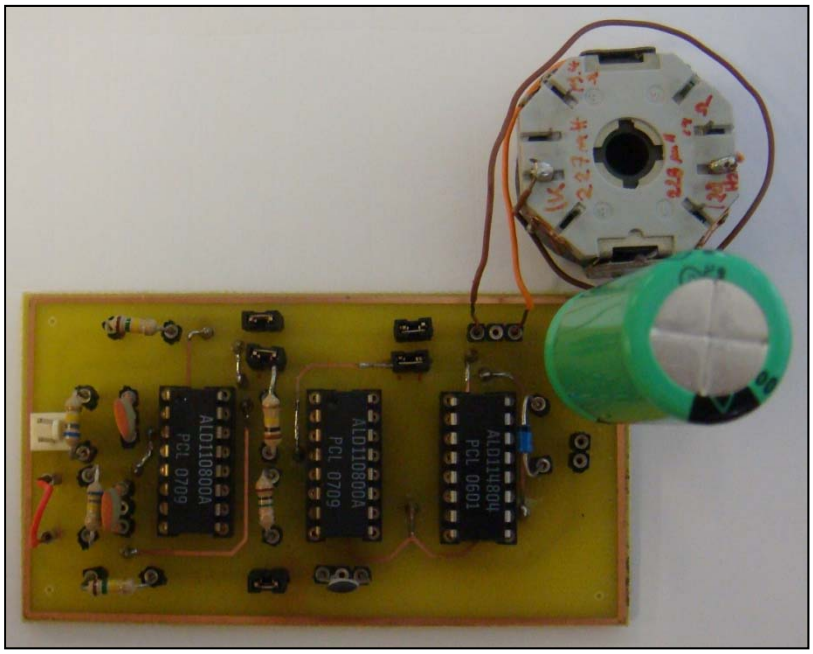

Figure 25 - Final PCB with the Oscillator and the Boost Converter

The PCB is composed by three parts, also known as stages, each one separated from the others, namely in terms of sign and feeding voltage. In Figure 26 we can see the three stages of the PCB marked inside boxes. It is also marked the input and output pins and the jumpers that will allow signal and voltage to reach each of the stages.

Figure 26 - PCB Stages and Parts

The first stage is the astable oscillator. It produces a theoretical square wave with a frequency of about 2 KHz. In practice the wave has a frequency of about 2 KHz and is not as square as expected (see Figure 27). To avoid the not so square wave and change it to an almost square wave, a second stage is needed and a buffer was used. This buffer is also composed by EPAD MOSFETs from ALD and it is a MOSFET in an inverter configuration. The output waves can be seen in Figure 28.

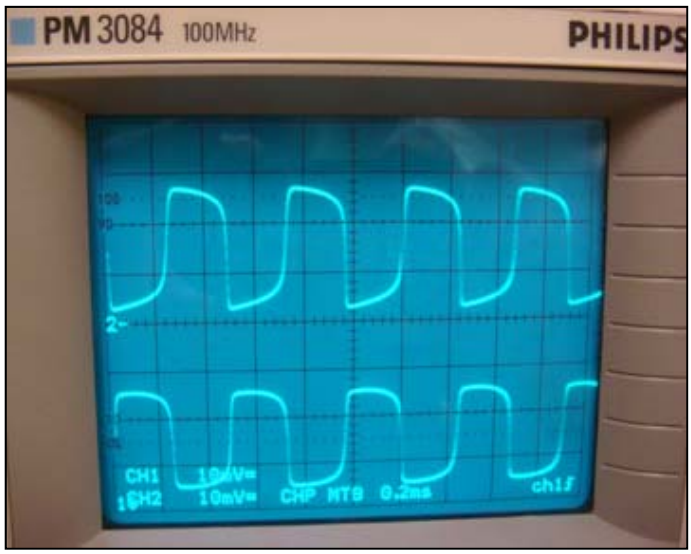

Figure 27 - Waves at the Oscillator Outputs

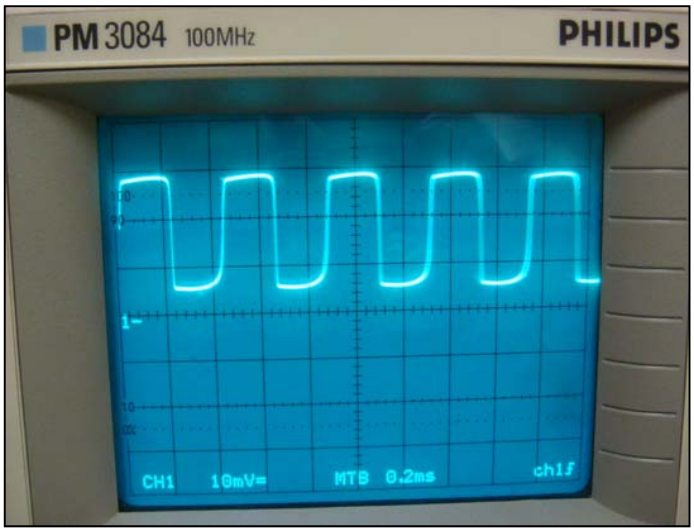

Figure 28 - Almost Square wave at the Buffer exit

Regarding the current consumption, tests were done to estimate the amount that is consumed in the first stage, by the oscillator, and on the second stage, with the oscillator combined with the buffer.

To start, the oscillator was tested alone without any kind of load with a lab temperature of about 29^{o}C, and the results can be seen on Table 3.

Vin(V)	Voutmin(V)	Voutmax(V)	Iconsumed(A)	Frequency(Hz)
0,2	0,06	0,16	0,0000012	3571
0,3	0,04	0,26	1,90E-06	2326
0,4	0,04	0,35	2,60E-06	1786
0,5	0,04	0,44	3,30E-06	1538
0,6	0,02	0,52	4,00E-06	1087
0,7	0,02	0,62	4,80E-06	1250
0,8	0,02	0,72	5,60E-06	1190
0,9	0,02	0,8	6,40E-06	1136
1	0,02	0,88	7,20E-06	1111
1,1	0,02	1	8,00E-06	1042
1,2	0,02	1,08	8,80E-06	1020
1,3	0,02	1,18	9,60E-06	1000
1,4	0,02	1,24	1,03E-06	980
1,5	0,02	1,36	1,11E-06	962

Table 3 – Oscillator Test Results

The tests start at 0,2V because below that there is no signal on the output. As it can be seen, the frequency decreases as the input increases, due to the internal capacitors of the EPAD MOSFETs. Regarding the current consumption, this oscillator has a very low current consumption as it can also be seen at Table 3. As the oscillation was not a perfect square wave, a buffer was implemented to make the wave squarer and the same tests for frequency and current consumption were done. The results are presented in Table 4.

Vin(V)	Voutmin(V)	Voutmax(V)	Iconsumed(A)	Frequency (Hz)
0,2	0,09	0,18	1,80E-06	3846
0,3	0,06	0,29	2,70E-06	2500
0,4	0,04	0,3	3,70E-06	1923
0,5	0,04	0,48	4,70E-06	1613
0,6	0,04	0,58	5,70E-06	1429
0,7	0,04	0,68	6,70E-06	1316
0,8	0,04	0,78	7,60E-06	1220
0,9	0,04	0,88	8,60E-06	1163
1	0,04	0,98	9,60E-06	1136
1,1	0,04	1,08	1,05E-05	1087
1,2	0,04	1,16	1,15E-05	1064
1,3	0,04	1,24	1,25E-05	1042
1,4	0,04	1,36	1,35E-05	1020
1,5	0,04	1,44	1,45E-05	1000

Table 4 - Oscillator + Buffer Test Results

As showed on Table 4, the current consumption did not rise to high levels, which is a very good signal. Taking into account that the oscillator and the buffer together only consume about 2,7uA, with an input of 300 mV, it can be stated that this is the right solution.

Having an almost perfect square wave at the buffer exit and a slight offset, this can be used in the switching MOSFET of the pre-boost converter.

4.2 Pre-Boost and Power Boost Converters

Power can be atained from all sorts of things, but in this specific case it comes from DC sources such as batteries, solar panels, rectifiers, and DC generators. A process that changes one DC voltage to a different DC voltage is called DC to DC conversion. A boost

converter, Figure 29, is a DC to DC converter with an output voltage greater than the source voltage. And it is also called a step-up converter since it “steps up” the input voltage. Since power ($P = VI$) must be conserved, the output current is lower than the source current.

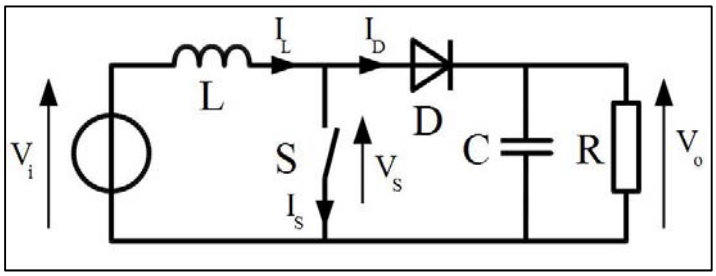

Figure 29 - Boost Converter - Simplified Model

The main principle that makes the boost converter works is the tendency of an inductor to resist changes in current. While being charged, it acts as a load and absorbs energy (somewhat like a resistor) and when being discharged, it acts as an energy source (somewhat like a battery). The voltage it produces during the discharge phase is related to the rate of change of current, and not to the original charging voltage, thus allowing different input and output voltages.

The basic principle of a Boost converter consists in two distinct states, Figure 30:

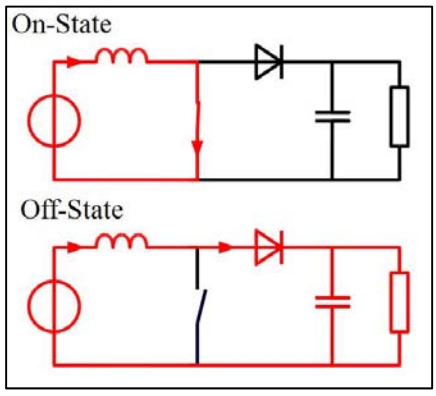

Figure 30 - Boost Converter - The 2 distinct states

When the converter is in the On-state, the switch is closed, resulting in an increase of current in the inductor.

For the Off-state, the switch is open and the only path offered to inductor current is through the flyback diode D, the capacitor C and the load R. This results in transferring the energy accumulated during the On-state into the capacitor.

The input current is the same as the inductor current, as can be seen in Figure 30 marked with a red trace. It is not discontinuous and the requirements on the input filter are simpler compared to other circuits like the buck converter, for instance.

When a boost converter operates in continuous mode, the current through the inductor (I_L) never falls to zero. Figure 31 shows the typical waveforms of currents and voltages in a converter operating in this mode.

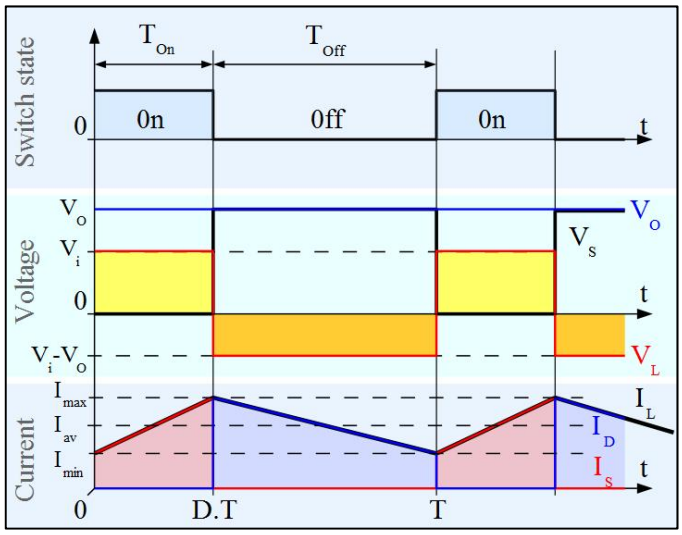

Figure 31 - Waveforms of current and voltage in a boost converter operating in continuous mode

The output voltage can be calculated as follows, in the case of an ideal converter (i.e. using components with an ideal behavior) operating in steady conditions:

During the On-state, the switch S is closed, which makes the input voltage (V_i) appear the inductor's extremes, which causes a change in current (I_L) flowing through the inductor during a time period (t), given by the formula:

$$\frac{\Delta I_L}{\Delta t} = \frac{V_i}{L} \qquad (4.2.1)$$

At the end of the On-state, the increase of I_L is therefore:

$$\Delta I_{L_{ON}} = \frac{1}{L}\int_0^{DT} V_i dt = \frac{DT}{L}V_i \qquad (4.2.2)$$

D is the duty cycle. It represents the fraction of the commutation period T during which the switch is On. Therefore D ranges between 0 (S is never on) and 1 (S is always on).

During the Off-state, the switch S is open, so the inductor current flows through the load. If we consider that there is no voltage drop in the diode, and the capacitor is large enough for its voltage to remain constant, the evolution of I_L is:

$$V_i - V_o = L\frac{dI_L}{dt} \qquad (4.2.3)$$

Therefore, the variation of I_L during the Off-period is:

$$\Delta I_{L_{OFF}} = \int_0^{(1-D)T} \frac{(V_i - V_o)dt}{L} = \frac{(V_i - V_o)(1-D)T}{L} \qquad (4.2.4)$$

As we consider that the converter operates in steady-state conditions, the amount of energy stored in each of its components has to be the same at the beginning and at the end of a commutation cycle. In particular, the energy stored in the inductor is given by:

$$E = \frac{1}{2}LI_L^2 \qquad (4.2.5)$$

Therefore, the inductor current has to be the same at the beginning and the end of the commutation cycle. This can be written as:

$$\Delta I_{L_{ON}} + \Delta I_{L_{OFF}} = 0 \qquad (4.2.6)$$

Substituting $\Delta I_{L_{ON}}$ and $\Delta I_{L_{OFF}}$ by their expressions yields:

$$\Delta I_{L_{ON}} + \Delta I_{L_{OFF}} = \frac{ViDT}{L} + \frac{(V_i - V_o)(1-D)T}{L} = 0 \qquad (4.2.7)$$

This can be written as:

$$\frac{V_o}{V_i} = \frac{1}{1-D} \qquad (4.2.8)$$

This in turns reveals the duty cycle to be:

$$D = 1 - \frac{V_i}{V_o} \qquad (4.2.9)$$

From the above expression it can be seen that the output voltage is always higher than the input voltage (as the duty cycle goes from 0 to 1), and that it increases with D, theoretically to infinity as D approaches 1. This is why this converter is sometimes referred to as a *step-up* converter.

Taking in consideration this theoretical approach, the boost converter on the PCB (see Figure 25 and Figure 26) can be tested.

The tests consisted on applying input tensions from 0,2V to 1V, since this is an application designed to low or ultra low voltage, and measure the consumed current and the output voltage with no load and with loads from 10 MΩ to 10 KΩ.

Vin(V)	Vout(V)	Iconsumed(A)
0,2	0,2	1,70E-04
0,3	1,15	2,10E-04
0,4	2,4	2,50E-04
0,5	4,2	2,90E-04
0,6	5,8	3,40E-04
0,7	8	3,90E-04
0,8	9,8	4,50E-04
0,9	11,8	5,10E-04
1	13,5	5,80E-04

Table 5 - Boost Converter Test - No Load

The first test was made without any load. The results are presented in Table 5. Analyzing the current consumption, it increased due to the inductor of the Boost Converter and its energy storage. Regarding the output tension, with no load, it has some good values, but for the inputs that are intended to it is still too low. For instance for 300 mV and 400 mV there is only about 1V to 2V available, not even half of the 5V needed, and these values, as stated, are with no load.

		Boost w/10M		**Boost w/1M**
Vin(V)	Vout(V)	Iconsumed(A)	Vout(V)	Iconsumed(A)
0,2	0,24	1,84E-04	0,2	1,85E-04
0,3	1	2,20E-04	0,8	2,22E-04
0,4	2,3	2,59E-04	2	2,61E-04
0,5	3,9	3,03E-04	2,6	3,05E-04
0,6	5,4	3,49E-04	3,6	3,53E-04
0,7	6,8	3,95E-04	4,5	3,99E-04
0,8	8,4	4,44E-04	5,9	4,48E-04
0,9	10,4	4,99E-04	6,4	5,03E-04
1	12	5,60E-04	8	5,63E-04

Table 6 - Boost Converter Test - 10 MΩ and 1 MΩ Loads

Despite the bad results of the tests with no load, other tests were done with some loads to get an idea of the output current. The Table 6 shows the output voltage and consumed current results to the Boost Converter with a load of 10MΩ and 1MΩ. Those are low loads, so the values for 300mV and 400 mV did not change much. For a load of 1 MΩ the changes for those values have started to decrease, and will continue decreasing while the load becomes higher (lower resistance) as it can be seen in Table 7.

		Boost w/ 100K		Boost w/10K
Vin(V)	Vout(V)	Iconsumida(A)	Vout(V)	Iconsumida(A)
0,2	0,15	1,86E-04	0,1	1,93E-04
0,3	0,43	2,25E-04	0,24	2,42E-04
0,4	0,86	2,68E-04	0,4	2,89E-04
0,5	1,25	3,14E-04	0,52	3,40E-04
0,6	1,65	3,64E-04	0,76	4,18E-04
0,7	2	4,13E-04	0,96	4,82E-04
0,8	2,45	4,65E-04	1,16	5,50E-04
0,9	3	5,23E-04	1,36	6,25E-04
1	3,5	5,89E-04	1,7	7,09E-04

Table 7 - Boost Converter Test - 100 KΩ and 10 KΩ Loads

For loads of 100KΩ and 10KΩ the output values for 300 mV and 4 mV are very low, for 10KΩ the boost converter only starts to boost the input tension from 500 mV and above.

The conclusion that can be taken from these tables and observations is that this Boost Converter does not provide enough output current that can drive a high load like the 10KΩ. This can be due to many things, but the most notorious is the EPAD MOSFETs drive capability, which is below the expectations.

Due to not being able to drive high loads, this initial stage will be used as a startup circuit for a power stage.

4.3 Schmitt Trigger – The Delay and Buffer Circuits

This block has implemented a circuit that delays the power source and input voltage of the Texas Instrument Buffer. It is composed by a resistor and a capacitor. While the

capacitor charges through the resistor, it delays the start of the next circuit. It is also a way to enable a sufficient charge in the pre-boost capacitor to achieve the necessary voltage to allow the perfect start of the following stage.

The Schmitt-trigger buffer is operational at 0.8-V to 2.7-V VCC, but is designed specifically for 1.65-V to 1.95-V VCC operation. The SN74AUC1G17 from Texas Instruments contains one buffer and performs the Boolean function Y = A, as described in Figure 32. The device functions as an independent buffer, but due to the Schmitt action, it may have different input threshold levels for positive-going (VT+) and negative-going (VT−) signals (37).

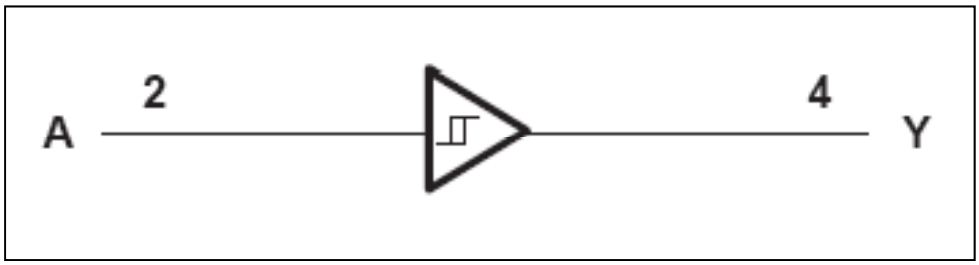

Figure 32 – Schmitt Trigger Buffer Logic Diagram (Positive Logic)(37)

Regarding the practical part, the charging time will vary with the capacitor value. It only consumes about 5uA, as described in the documentation.

4.4 Schmitt Trigger Oscillator

This Schmitt-trigger inverter is operational at 0.8-V to 2.7-V VCC, but is designed specifically for 1.65-V to 1.95-V VCC operation. The SN74AUC1G14 contains one inverter and performs the Boolean function Y = A, as described in Figure 33 . The device functions as an independent inverter, but due to the Schmitt action, it may have different input threshold levels for positive-going (VT+) and negative-going (VT–) signals (36).

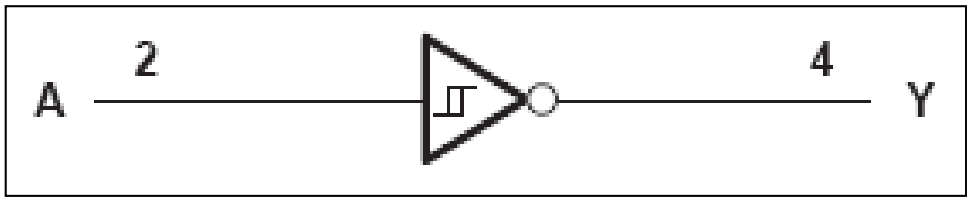

Figure 33 - Schmitt Trigger Inverter Logic Diagram (Positive Logic)(36)

The inverter characteristics of this Schmitt Trigger are very useful. The oscillator that will attack the power boost converter is made with this Schmitt Trigger(Figure 34).It is also represented a capacitor and a pull up resistor to increase positively the oscillation offset to reach a maximum value of about 1V to attack with a higher value the gate of the power MOSFET.

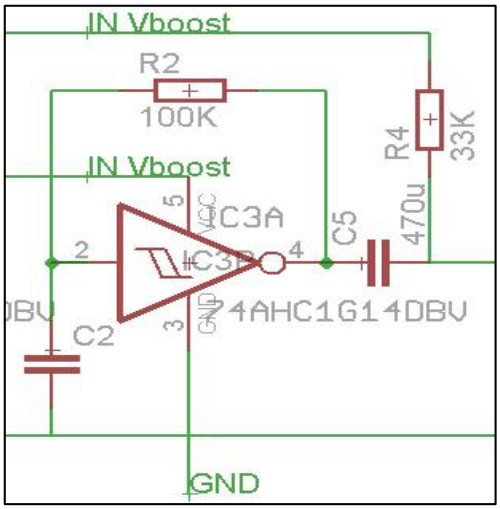

Figure 34 - Oscillator Circuit with the Schmitt Trigger Inverter and the pull up capacitor and resistor

At the Inverter Schmitt Trigger exit it can be seen a perfect square waves, (Figure 35). At this stage exit, before attacking the power MOSFET gate, the square wave's offset will be pulled up so the signal can have more strength to attack de MOSFET's gate, (Figure 36).

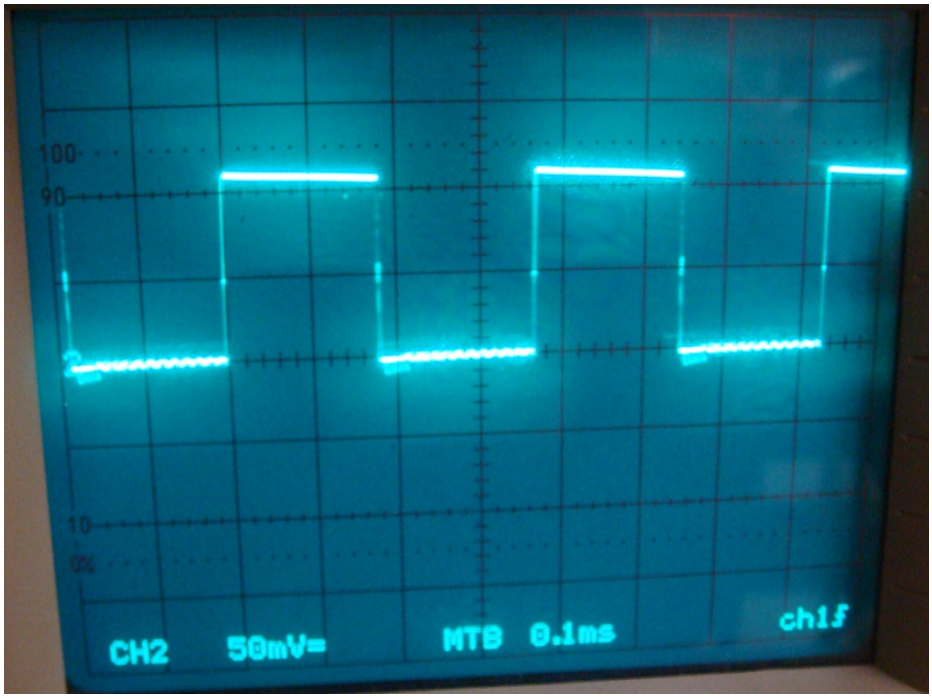

Figure 35 - Square wave at the Inverter Schmitt Trigger exit

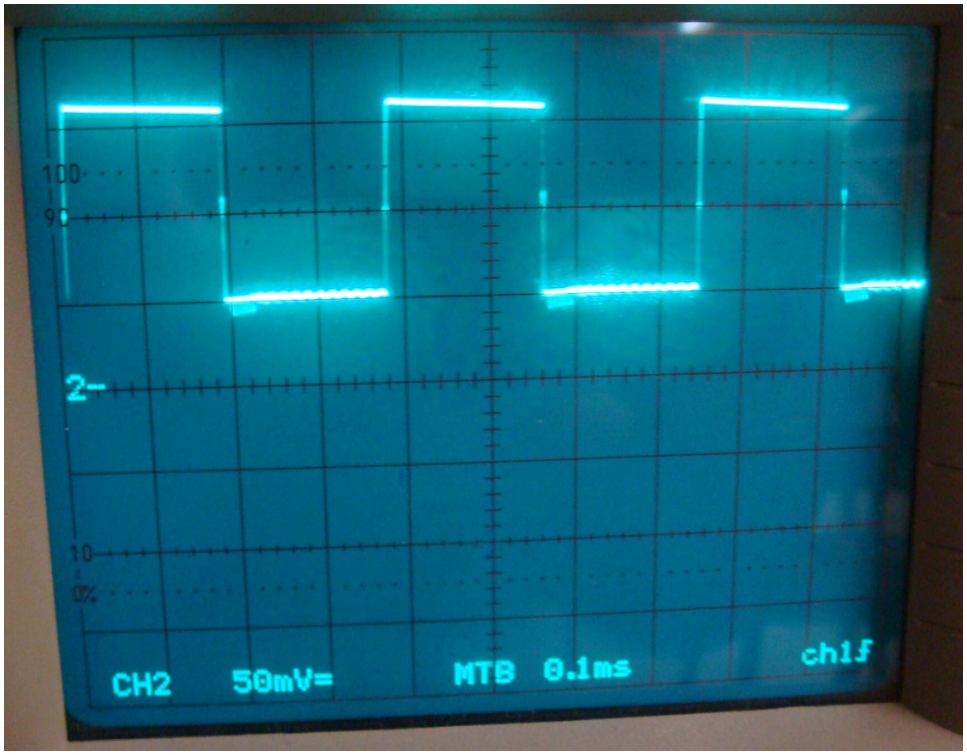

Figure 36 - Square wave's offset increased

4.5 Ultra Low Voltage Circuit

Before the beginning of the final tests, the Ultra Low Voltage circuit was assembled in a bread board. Assembling all the pieces together allow to rearrange certain aspects related to the timing of charge of some capacitors, for instance the one that is in the delay circuit, and the power boost converter frequency or inductance, that needed a little adjustment to work with the exact amplitude and offset provided by the Schmitt Trigger oscillator to, at the end, provide more power and therefore more efficiency.

Regarding the capacitor present in the delay circuit, it needed to have a reset button. It was observed that when the first boost converter starts to charge the output capacitor, if the delay capacitor had charge it starts instantaneously to feed the Schmitt Triggers stages. To solve this problem a reset button was placed, needing to be pressed every time that that circuit is powered on.

The frequency of the power boost converter was tested with a signal generator. These tests provided good information about the power MOSFET's gate threshold voltage, which is between 0,4V and 0,9V as stated in the datasheet. The gate threshold voltage value was indeed inside that range, in this case, with a drain voltage of about 0,4V and it needed about 0,7V to switch on.

Various values of inductances were measured and, in the end, it was chosen an inductance with about 2,4mH and 1,9 Ω. This inductance was chosen among the others because it produced, at the Power Boost converter exit, an output voltage of about 4,2V with a 10KΩ charge and it only consumed 6mA. This inductance was the only one to consume a current bellow 10mA and to produce such high output voltage.

To finalize the Power Boost converter tests, a duty cycle and offset tests were done. Regarding the duty cycle, no important changes where noticed, but for the offset it was observed that an increase of about 500mV was enough to gain an extra 0,6V at the power boost converter exit, if the offset exceed that value, the output decreased drastically. To solve this problem a capacitor and a pull up resistor were placed between the Schmitt Trigger Oscillator and the power MOSFET.

For the final tests, printed circuit boards (PCB) where done to avoid certain losses and parasite capacities of the bread boards. The final PCB's can be seen in Figure 37. The a) in Figure 37 is the first Stage of the Ultra Low Voltage Circuit it is the Ultra Low Voltage Oscillator with the Pre-Boost Converter and its handmade inductor. The b) group in Figure 37 is the second Stage of the Ultra Low Voltage Circuit, the Schmitt Triggers buffer and Oscillator and the Power Boost Converter.

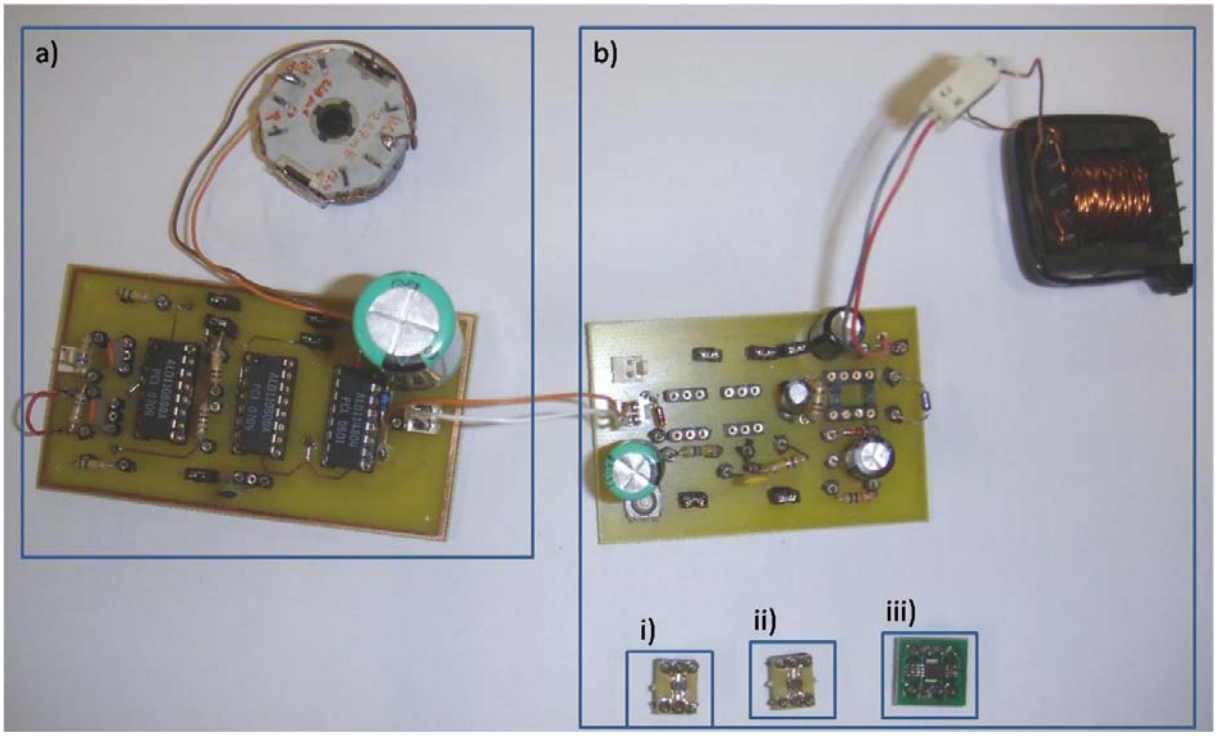

Figure 37 - Final PCB's - a) Ultra Low Voltage Oscillator and Pre-Boost Converter; b) Schmitt Trigger Buffer and Oscillator and Power Boost Converter; b) i) Schmitt Trigger Buffer; b) ii) Schmitt Trigger Inverter; b) iii) Power MOSFET;

The result is an ultra low power oscillator that starts with an ultra low voltage of 400mV, and even down to 390mV, then a buffer to give strength and increase the offset of the oscillation signal offset to attack a pre-booster circuit that will charge until it reaches about 1.2V.

Meanwhile the delay circuit starts to charge and when it allows the output voltage of the pre-boost to reach the Schmitt Trigger oscillator, this with a pull up resistor so to increase the signal offset produces a square wave that will switch the power Boost circuit that will produce an output voltage of about 4.2V with a resistive load of 10KΩ.

The feedback diode will allow the final circuit to work a couple of seconds to prevent some input failures. It also allows the power boost output voltage to charge the capacitor of the pre-boost circuit allowing this to maintain a certain voltage or to reach a higher voltage.

4.6 Results

Considering that the main objective of this circuit is to increase the ultra low 400mV to a usable value consuming low current, the experiment results are presented in Table 8 and in Figure 38

The Table 8 shows the input voltage, consumed current, the output voltage achieved and the efficiency of the final circuit with a 10KΩ load.

Vin (V)	Vout (V)	I (A)	Efficiency
0,1	0	9,64E-05	0,00
0,2	0	1,95E-04	0,00
0,3	0	2,78E-04	0,00
0,4	4,2	8,09E-03	54,51
0,5	4,6	1,01E-02	42,03
0,6	4,6	1,22E-02	28,98
0,7	4,8	1,50E-02	21,99
0,8	4,8	1,72E-02	16,76
0,9	4,8	1,96E-02	13,07
1	4,8	2,20E-02	10,47

Table 8 - Final values of the Ultra Low Voltage Circuit with a 10KΩ load.

The output voltage values were acceptable, being the 4,2V with an input voltage of 0,4V (see Table 8) enough to drive an integrated circuit. On the other side, the consumed current is a little bit high for the requirements, but nevertheless it has an efficiency of about 54% which in this case, being this an analog solution is very good.

Another thing is that the circuit starts operating with an input voltage of 390mV and it produces about 4V with a current consumption of about 7,15mA, representing an efficiency of 57,4%.

If we take into consideration that the initial requirements were 0,4V and a current consumption of 1mA, achieving an output of 5V and, following the previous examples, using a 10KΩ load, the circuit had to have an efficiency of about 625% which was impossible to reach.

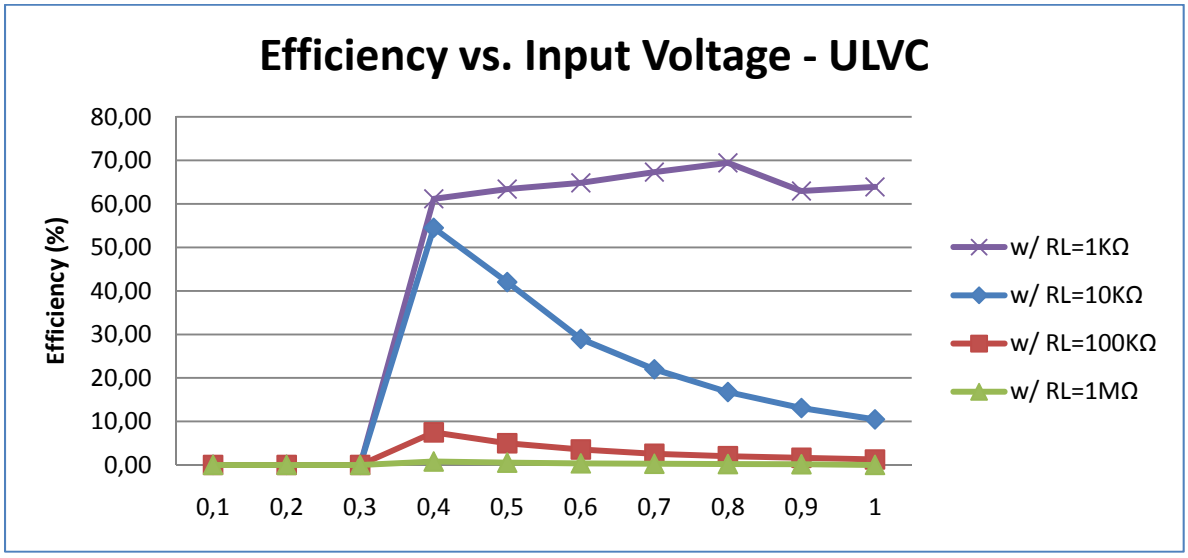

Figure 38 – Ultra Low Voltage Circuit- Efficiency versus Input Voltage

The Figure 38 shows the results with other loads, from 1KΩ to 1MΩ. It can be observed that as the load increases the efficiency also increases. This can be simply explained because there is no control duty-cycle and, for this reason, the energy supplied to the inductor is relatively constant and then dissipated on the load resistor or anywhere else.

4.7 Ultra Low Voltage Circuit vs. ST L6920

This subchapter aims to compare the developed solution with one other available already in the market circuits, such as the integrated circuit of ST, the L6920.

Regarding the results for the commercial solution, it can be said that it starts bellow the value that the datasheet indicates. More precisely it starts with an input tension of about 0,9V, although the range described in the datasheet about 1V. Regarding the consumed current it can be seen in Table 9, it rises when the integrated starts to work, tending to stabilize afterwards. This can also be seen by the output voltage that increases from 1V to 5,2V in a range of 200mV.

Vin (V)	Vout (V) Rl=10K	I (A)	Efficiency w/ RL=10KΩ
0,4	0	9,60E-08	0,00
0,5	0	5,12E-06	0,00
0,6	0,12	1,31E-05	18,36
0,7	0,7	7,37E-05	94,93
0,8	1	7,20E-03	1,74
0,9	5,2	6,22E-03	48,30
1	5,2	5,50E-03	49,16

Table 9 - ST L6920 Output Voltages, Consumed Current and Efficiency for a 10KΩ load.

The Figure 39 shows the efficiency of the L6920 with other load values, from 1KΩ to 1MΩ.

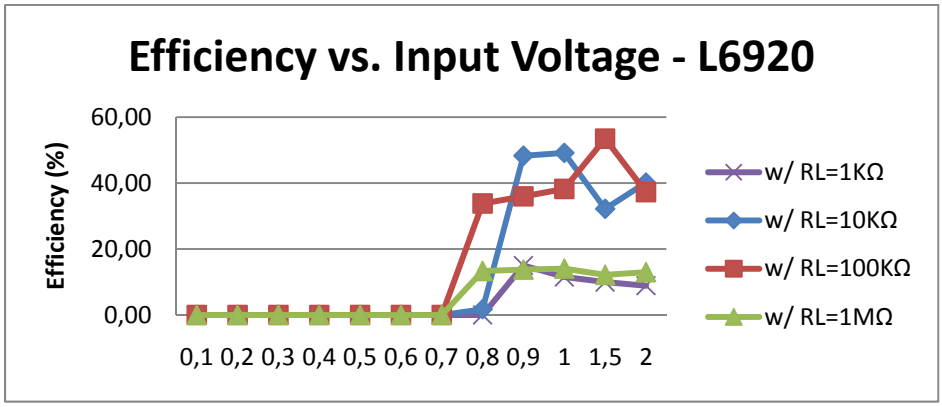

Figure 39 - ST L6920 - Efficiency versus Input Voltage Graphic with loads from 1KΩ to 1MΩ.

The drop that occurred with an input voltage of 0,9V is due to the activation of the device. The integrated circuit starts to consume more current than when it is stable and that is observed with an input voltage greater than 0,9V, when the output voltages reaches its maximum value 5V.

To compare the two solutions, the one presented in this document and the solution proposed by ST Microelectronic's L6920, a load of 10KΩ was chosen. The Figure 40 shows that the solution proposed by this work, with a load of 10KΩ, is indeed more efficient for lower input voltages. Nevertheless the L6920 does consume less current, (Figure 41), which means an increased efficiency for higher input voltages.

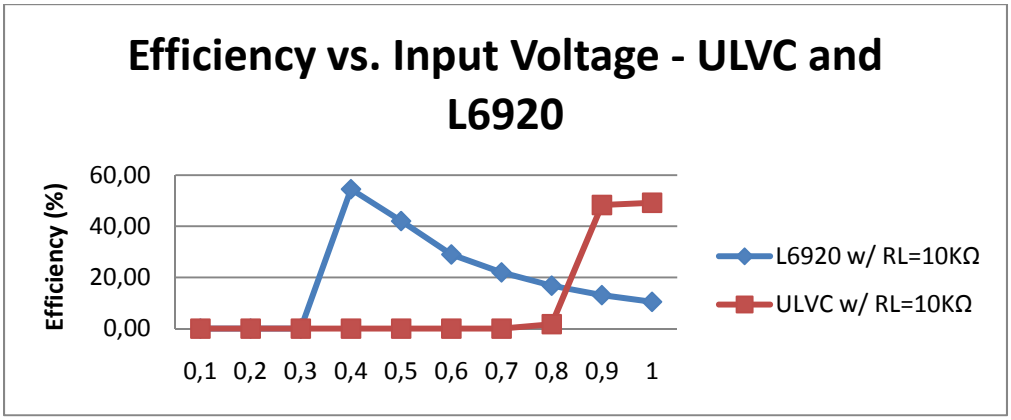

Figure 40 - ULVC and L6920 Efficiency comparison for a 10KΩ load.

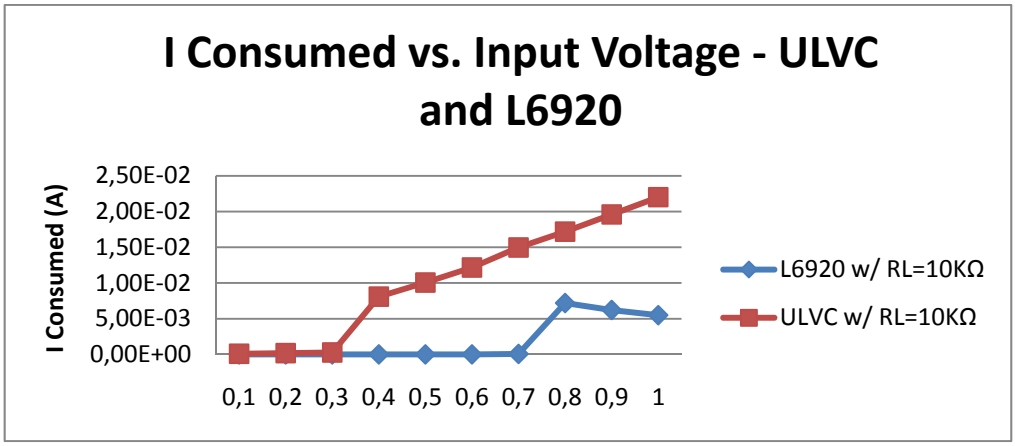

Figure 41 - ULVC and L6920 Consumed Current comparison for a 10KΩ load.

To finalize this analysis Figure 42 shows the output voltage of the both circuits. The ULV Circuit has a lower output voltage, but it reaches it faster than the L6920 and it has a lower startup voltage than the L6920.

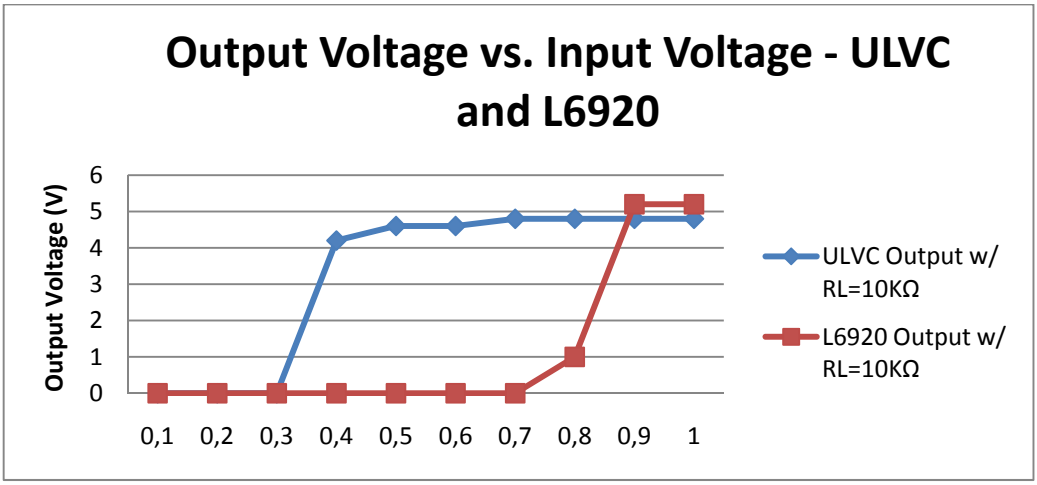

Figure 42 - ULVC and L6920 Output Voltage comparison for a 10KΩ load.

The ST Microelectronics L6920 has a higher output voltage, but it takes longer to reach its maximum potential and the startup voltage is not low enough to make this a good solution to the main problem of this work.

4.8 Conclusions

This Chapter presented the developed work. Each block was observed in detail, and the final solution was confronted with the best commercial solution that was found previously.

The starter circuit allows it to start with a voltage bellow the maximum 400mV available and it can increase the input voltage to 4,2V, which is a value that can be used to power some external hardware that could not be powered with the available 400mV or less.

It also has a feedback diode that allows it to achieve a higher attack signal at the power MOSFET's gate. This part still needs some work done to make all the circuit autonomous for a while when the input voltage fails.

The only parameter where this solution fails is in the current consumed. It is a determinant factor, since there is only 1 mA available. This solution consumes about 8mA, thus making it no suitable for the target project unless the optical power is increased. Meanwhile there are other systems where this solution can be viable, such as some solar panels. Small Photovoltaic Panels can provide power enough to this device, and because this is a device that works with low voltage, it enables the panel to work longer since it will be able to provide some power even when there is not enough light for the panel to have its full efficiency.

The ST Microelectronics integrated circuit L6920 is a good solution when more than 0,9V input voltage is available, since it is the minimum startup voltage that can make the integrated circuit work. Provided this, the device can work with fixed or an adjusted range of output voltages, consuming low current, therefore with high efficiency. It is also an easy to implement solution due to low number of components needed to its operation. The reduced size is also something to take into account when developing portable systems.

In conclusion, it can be said that the ULV Circuit solution satisfy almost all the required parameters. Being able to start its operation with ultra low voltages and provided an output voltage value high enough to power cheap off-the-shelf electronics.

Chapter 5: Ultra Low Voltage Source – Germanium approach

Existing boost circuits can start up and drain a power source down to 1 V, but that still leaves too much unusable energy in a battery or in whatever storage system. Other power sources, like solar cells or micro-turbines, need circuitry to start up at much less than 1 V. For instance, a single solar cell has a full-sun output of about 0.6 V, depending on the dimensions.

The circuit that will be proposed targets this problem. It performs a dual-inductor step-up conversion at a startup voltage almost as low as 200 mV. An inductive dc-dc boost circuit outputs to a higher voltage than its input. A germanium-transistor balanced-boost circuit is simple, using only two NPN, and also a version with two PNP transistors, but it unconditionally starts at a very low voltage. Previous commercial silicon-transistor boost circuits required approximately a volt to start and many more components.

5.1 The Germanium Transistors

Being an almost extinct technology, the germanium transistors were and still are, in some applications, an alternative to the modern transistors.

In their time, early plastic-encapsulated transistors were unreliable. Moisture and impurities, trapped during the encapsulation process, "poisoned" the germanium heart of the transistor. This slow killing process caused unstable operation and failure. Several important facts were learned during the evaluation of plastic-coated transistors. First,

transistors must be assembled under surgically clean conditions. Second, rigorous factory tests were necessary if quality and performance were to be maintained. Third, the units had to be enclosed in hermetically sealed containers. For example, transistors encapsulated in plastic had relatively large I_{co} and I_{cbo} readings. When the same units were assembled under surgical conditions and mounted in hermetically sealed cases, these current readings dropped appreciably.

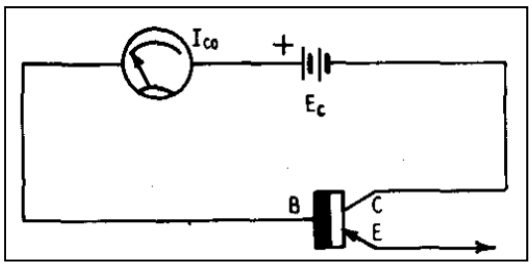

Figure 43 - Measuring dc Leakage current between collector and base. Emitter is open circuited;(38)

The I_{co} reading (Figure 43) for most hermetically sealed, small-signal transistors should be less than 18 Amp at room temperature, with -22.5 Volts between collector and base. The manufacturer of 2N43 and 2N43A p-n-p transistors specifies that I_{co} shall be less than 10 Amp at room temperature, with -45 volts between collector and base. This should become an industry-wide standard.

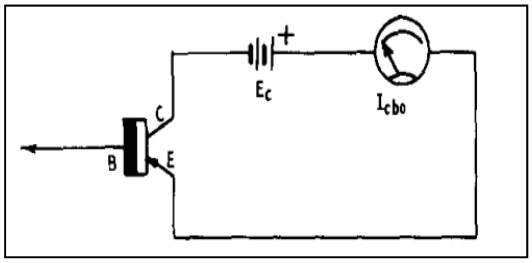

Figure 44 - Measuring dc leakage current between collector and emitter. Base is open circuited;(38)

The I_{cbo} reading (Figure 44) for most hermetically sealed, small-signal transistors should be less than 125 A at room temperature, with -6 volts between collector and emitter. Both I_{cbo} and I_{co} increase when a warm soldering iron is held near a transistor or even if the

unit is held in the fingers while making measurements. This is another way of emphasizing that current increase with temperature. It is illustrated in graphs of I_{co} versus temperature on data sheets that accompany most transistors. If current increases slightly with temperature, there is no cause for alarm unless the current is unsteady. This often means defective junctions (38).

5.2 Germanium Dual Boost Circuit

The circuit that is now purposed aims to solve the problem of the startup voltage. It should start its operation with about 400 mV or less.

Despite there are many models of germanium transistors, in this test were used only four different models, one NPN and 3 PNP. The NPN AC127 and the PNP AC188 were used to test the circuit functionality. For the remaining, since it is easier to find PNP germanium transistors, the 2SA30 and the OC1045 were chosen. The main choice factors were the bias current and the transistor gain, hfe. For the bias current those with the minor value were chosen and for the gain those with the highest value. Since these two parameters are not independent, it was tried to achieve a balance point, not to gage any of the parameters.

5.2.1 NPN Germanium Transistors – AC127

The first germanium transistor to be tested was the NPN type, the AC127. The Figure 17 shows the dual boost circuit with the NPN transistors.

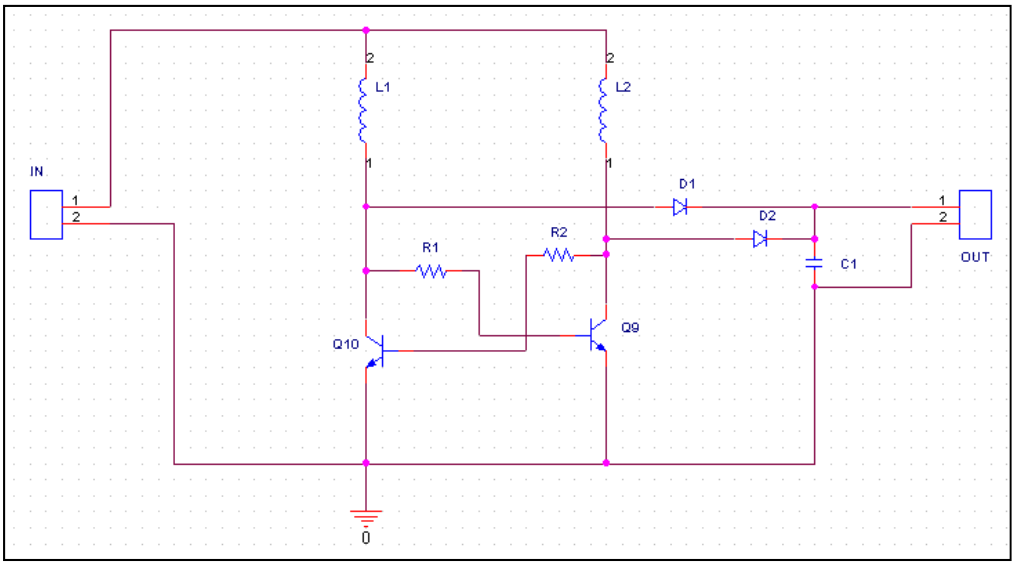

Figure 45 - NPN Germanium Transistor Dual Boost

The circuit operates like a free-running multi-vibrator. The repetitive cycle starts with V_{in} slightly above Q9's V_{be} creating a positive Q9 base current (I_b = (V_{in} - V_{be})/R1) flowing through L1, and Q9 turns on, which switches inductor L2 to ground. Q10 is off, and L1's current flow is very small. D1 and D2 are off. Energy stored within L2's magnetic field builds as L2's current rises with a positive di/dt and as this current rises, it also flows through Q9's R_{sat}. When Q9's collector voltage becomes sufficiently large to turn on Q10, R2 connects Q10's base voltage to Q9's collector, and also limits Q10's base current.

With Q10 turning on, the previous base drive to Q9 is now shunted to ground, and Q9 turns off. Switching off Q9 allows L2's flyback energy to forward-bias D2 and flow into the load (R3) as L1's magnetic field collapses. D1 remains off. With L2 discharged, D2 turns back off. L1's magnetic field has been building as L1's current rises with a positive di/dt. This current flows through Q10's R_{sat}. Q10's collector voltage becomes sufficiently large to turn on Q9. Q9's base voltage is connected to Q10's collector by R1, which also limits Q9's base current.

With Q9 turning on, the previous base drive to Q10 is now shunted to ground, and Q10 turns off. Switching off Q10 enables L1's flyback energy to forward-bias D1 and flow into the load (R3) as L1's magnetic field collapses. D2 remains off. With L1 discharged, D1 turns off.

This self-oscillating action repeats until the input voltage falls below Q10's or Q9's V_{be}. As the input voltage increases, the stored energy in L1 and L2 increases, and thus the average voltage on also R3 increases.

The inductance of L1 and L2, the R_{sat} of Q10 and Q9, and the switching characteristics of Q10 and Q9 determine the period and duty cycle of the self-oscillation. The circuit can be optimized for a specific load and input source with adjustments to both L and R.

The advantage of this dual-boost configuration versus a single-ended boost configuration is that the output ripple contains lower noise and the input source is not off during flyback. For a solar cell or micro-turbine input, an off cycle is less than optimal.

This circuit, for an input as low as 300mV, achieved, with no load, an output voltage of almost 5V, consuming near 11.3 mA, with R1 and R2 equal to 330 Ωs. The frequency is near 45Hz. Optimizing this circuit changing the base resistors to 47 KΩ, it achieved an output voltage of 550 mV, consuming 1,3 mA with a frequency of about 9600Hz.

Since these germanium transistors have a high current consumption it was decided to put them aside because if we tried to optimize further the current consumption it would decrease but the output voltage and that has no interest for this work.

5.2.2 PNP Germanium Transistors

The test circuit for the PNP transistors is the same as the previous but with the references changed as show in Figure 46.

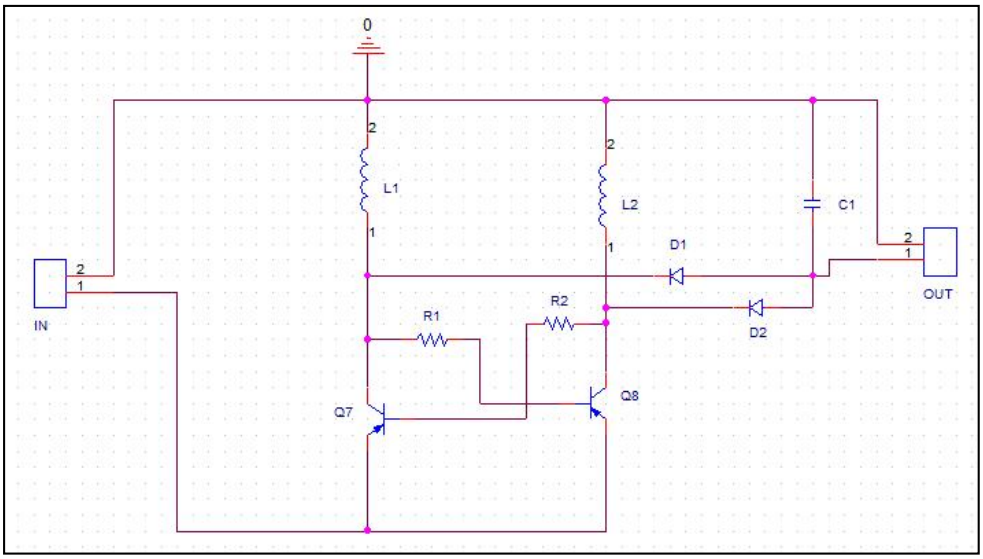

Figure 46 - PNP Germanium Transistor Dual Boost

- ***AC188***

Using AC188 germanium transistors in Q7 and Q8, just to test the circuit functionality with PNP transistors, with an input voltage of 300mV and no load, an output voltage of 3V was achieved with a current consumption of almost 6.2 mA and a frequency of 47Hz. The measures were made using R1 e R2 equal to 330 Ωs. Optimizing the base resistors to 47 KΩ an output voltage of 400 mV was achieved consuming 0,7 mA with a frequency of about 2600 Hz.

- ***2SA30***

These germanium transistors have an average small signal Forward Current Gain, hfe, of 250 (V_{ce}=3 V and I_c=1mA) and an average I_{cbo} equal to 0.2uA.

Being the test conditions the same as the ones for the AC188, base resistors equal to 330 Ωs and with no load, an output voltage of about 1,08 V was obtained with a current consumption of 2,8 mA and a frequency of 208 Hz.

Optimizing the base resistors to 3,3 KΩs, an output voltage of 1,7 V was obtained with a current consumption of 0,5 mA and frequency of about 500 Hz.

- ***OC1045***

These germanium transistors have an average hfe of 61 (V_{ce}=3 V and I_c=1mA) and an average I_{cbo} equal to 0.3uA. It were chosen to avoid undermining much of the current I_{cbo} at the expense of gain.

As the ones before this, the circuit was tested with an input tension of 300 mV, with no load, and base resistors equal to 330 Ωs. An output tension of 580 mV was obtained with a current consumption of 2,1 mA and a frequency of about 200 Hz.

After the optimization of the base resistors, putting these equal to 2,2 KΩ, with a current consumption of 0,5 mA an output voltage of 600 mV was obtained with a frequency of 2,7 KHz.

Since the tests done to all of the germanium transistors were with no load and only with one input voltage value, Table 10 to Table 13 shows the different values obtained with each one of the different germanium transistors for different input voltage values and with three different loads with an ambient temperature of about 28^{o}C.

AC127 Rb=47KΩ	Rload=10K		Rload=100K		Rload=1M	
Vin	**Vout**	**Iconsumed**	**Vout**	**Iconsumed**	**Vout**	**Iconsumed**
0,2	0,08	1,10E-03	0,14	1,30E-03	0,18	1,40E-03
0,3	0,16	1,70E-03	0,22	1,60E-03	0,39	1,80E-03
0,4	0,26	2,10E-03	0,54	1,80E-03	0,792	2,00E-03
0,5	0,34	2,40E-03	1,6	2,30E-03	2,4	2,20E-03
0,6	0,44	2,90E-03	2,15	2,50E-03	3,3	2,60E-03
0,7	0,54	3,30E-03	2,7	2,90E-03	3,7	2,80E-03
0,8	0,63	3,70E-03	3,2	3,00E-03	4,6	2,90E-03
0,9	0,72	4,40E-03	3,8	3,20E-03	5,4	3,20E-03
1	0,8	4,60E-03	4,6	3,30E-03	6,2	3,40E-03

Table 10 - NPN AC127 Output Voltages and Consumed Current for 10KΩ, 100KΩ and 1MΩ

AC188 Rb=47KΩ	10K		100K		1M	
Vin	**Vout**	**Iconsumed**	**Vout**	**Iconsumed**	**Vout**	**Iconsumed**
0,2	0,08	4,00E-04	0,17	4,00E-04	0,24	4,00E-04
0,3	0,21	4,00E-04	0,44	4,00E-04	0,6	4,00E-04
0,4	0,36	5,00E-04	0,73	4,00E-04	0,95	4,00E-04
0,5	0,49	5,00E-04	0,98	5,00E-04	1,35	5,00E-04
0,6	0,64	6,00E-04	1,26	5,00E-04	1,75	5,00E-04
0,7	0,78	6,00E-04	1,5	6,00E-04	2,15	5,00E-04
0,8	0,94	7,00E-04	1,8	6,00E-04	2,6	6,00E-04
0,9	1,08	7,00E-04	2	6,00E-04	3,15	6,00E-04
1	1,26	8,00E-04	2,3	7,00E-04	3,6	7,00E-04

Table 11 - PNP AC188 Output Voltages and Consumed Current for 10KΩ, 100KΩ and 1MΩ

2SA30 Rb=3,3KΩ	10K		100K		1M	
Vin	**Vout**	**Iconsumed**	**Vout**	**Iconsumed**	**Vout**	**Iconsumed**
0,2	0,2	3,00E-04	0,41	3,00E-04	0,59	3,00E-04
0,3	0,46	5,00E-04	0,94	5,00E-04	1,5	5,00E-04
0,4	0,72	7,00E-04	1,52	8,00E-04	2,35	8,00E-04
0,5	1,02	1,00E-03	2,15	1,00E-03	3,3	1,10E-03
0,6	1,3	1,30E-03	2,8	1,30E-03	4,3	1,40E-03
0,7	1,6	1,60E-03	3,45	1,60E-03	5,4	1,70E-03
0,8	1,9	1,90E-03	4,1	1,90E-03	6,3	2,00E-03
0,9	2,3	2,20E-03	4,7	2,20E-03	7	2,30E-03
1	2,6	2,50E-03	5,4	2,50E-03	7,6	2,60E-03

Table 12 - PNP 2SA30 Output Voltages and Consumed Current for 10KΩ, 100KΩ and 1MΩ

OC1045 Rb=2,2KΩ	10K		100K		1M	
Vin	**Vout**	**Iconsumed**	**Vout**	**Iconsumed**	**Vout**	**Iconsumed**
0,2	0,1	3,00E-04	1,80E-01	1,00E-04	0,25	2,00E-04
0,3	0,22	5,00E-04	0,4	4,00E-04	0,51	4,00E-04
0,4	0,35	7,00E-04	0,66	7,00E-04	0,8	7,00E-04
0,5	0,4	8,00E-04	0,9	9,00E-04	1,12	9,00E-04
0,6	0,65	1,00E-03	1,16	1,10E-03	1,5	1,10E-03
0,7	0,8	1,20E-03	1,4	1,30E-03	1,8	1,30E-03
0,8	1	1,40E-03	1,7	1,60E-03	2,1	1,60E-03
0,9	1,1	1,70E-03	1,9	1,80E-03	2,5	1,80E-03
1	1,2	2,10E-03	2,25	2,00E-03	2,8	2,00E-03

Table 13 - PNP OC1045 Output Voltages and Consumed Current for 10KΩ, 100KΩ and 1MΩ

As can be seen in the previous tables, these germanium transistors do not have a high efficiency since the current they consume is very high and the resulting output power is very low. For the NPN transistors the efficiency is about 1% to 3 %, for PNP transistors, the AC188 the efficiency reached the 11% but this is also a very low value, the 2SA30 reached

21%, the highest value of all the transistors, and finally the OC1045 reached 6%. Notice that besides the AC127 and the AC188, that have been tested with the same base resistors, all the others were tested with different base resistors chosen on the basis of minimum consumption of current and voltage at the output for each one of the transistor.

5.3 Conclusions

This chapter introduced the germanium transistors as an alternative source to the silicon-based transistors or to the switching MOSFETs of the normal boost converters, and the introduction of the dual boost circuit with these transistors.

Regarding the dual boost circuit it was demonstrated that this kind of transistors performs a dual-inductor step-up conversion with a input voltage as low as 200 mV, as for the normal silicon based transistors that have normal Base-Emitter voltages only start converting with input voltages above 0,7 V. This startup voltage of 200mV is very good compared with the other two solutions presented previously, the ST L6920 and the developed Ultra Low Voltage Circuit, with the startup voltages of 800mV and 390mV respectively.

About the results it can be said that the efficiency (

Figure 47) was too low for taking them in consideration. The output voltage (

Figure 48) was a little bit low in comparison with the other solutions presented previously. The germanium solution at maximum only provided 2,6V with a 10KΩ load, when the ULV Circuit and the L6920 reached easily at 4V and 5V respectively.

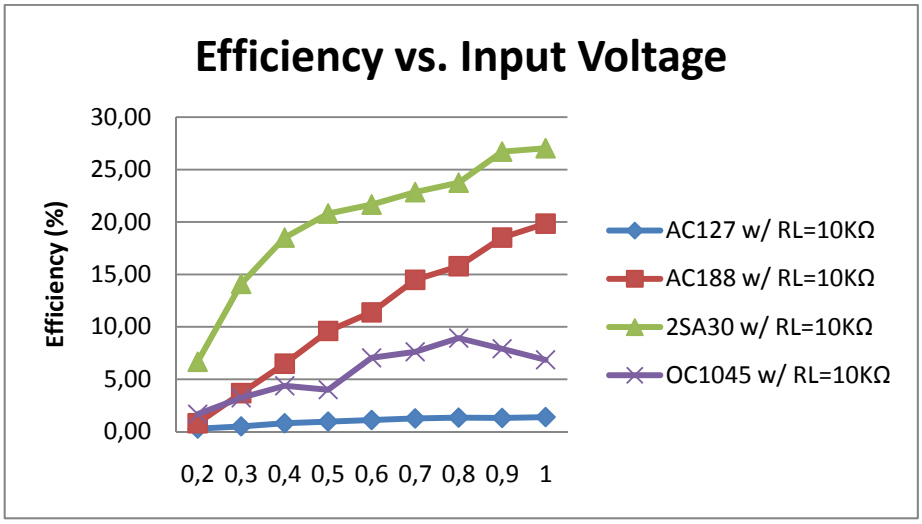

Figure 47 - Efficiency versus Input Voltage for each tested Transistor for a 10KΩ load.

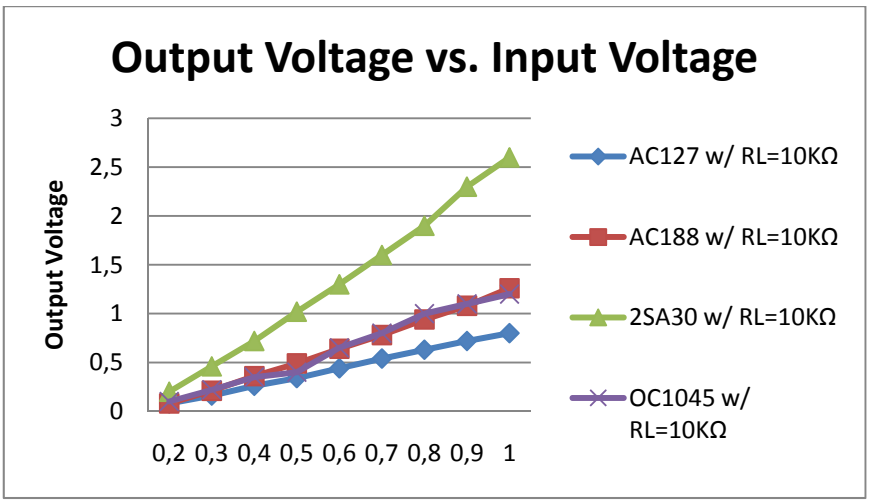

Figure 48 - Output Voltage versus Input Voltage for each tested Transistor for a 10KΩ load.

Other weak point of this kind of circuit is the current consumption. As can be seen in Figure 49, for a load of 10KΩ and to achieve an output voltage of about 2,6V it needs to consume about 2,5mA, which represents an efficiency of 27%. If we compare it once again with the other solutions, for about the same current consumption, we have efficiencies of about 54% for the L6920 and 10,5% for the ULV Circuit. It may seem that the germanium approach is better that the ULV Circuit developed, but the developed circuit has a startup efficiency of about 54% with an input voltage of 0,4V.

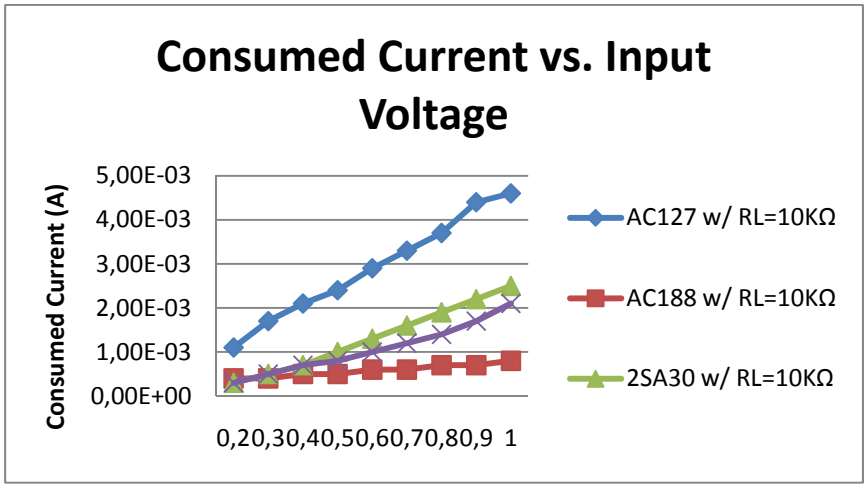

Figure 49 - Consumed Current versus Input Voltage for a 10KΩ load.

Finally, these germanium transistors have thermal runaway, meaning that their behavior will change with temperature. All the results were done with a laboratory temperature of about 28^{o}C but there are always some temperature variations, and that may be a reason for some variations in the results.

Chapter 6: Final Conclusions and Future Work

6.1 Final Conclusions

During this work it was studied, researched and implemented some different solutions (circuits) that could lead to a solution to the problem of increasing an ultra low voltage of 400mV to a useful value, consuming as less current as possible, being only available 1mA. None of them really solve the entire problem, as it is a rather difficult task as already stated.

The Ultra Low Voltage Circuit achieved an efficiency of about 54% which for an analog circuit as this one can be very good. The output voltage reached the 4,2V with the required input voltage of 0,4V with a consumed current of about 8mA. This circuit does startup with a little input voltage bellow the requirements, about 390mV, with an output tension of 4V and with a lower current consumption, about 7,15mA, which increases the efficiency of this circuit for 57,4%, (about 7% more efficient than with an input voltage of 400mV). All these values where obtained with a 10KΩ load, which means that it produces between 1,6mW and 1,7mW of power.

Regarding the integrated circuit L6920 from ST Microelectronics, it represented from the beginning a viable solution to the present problem. The only problem is the high startup voltage and this is one of the main requirements for the problem solution (a circuit that starts to work with an ultra low voltage of 400mV, or even lower if possible). L6920 has a startup voltage between 800mV and 900mV to produce 5V. Concerning the consumed current, in the previous conditions, it only consumed about 6,2mA which makes an efficiency of about 48%, an efficiency startup value a little lower than the ULV Circuit, but acceptable.

This integrated circuit from ST Microelectronics will also be a good solution to other harvesting technologies than the one discussed in this project.

To finalize, the Germanium approach. This presented the worst results, despite the various types and technologies of bipolar transistors. The efficiency of these circuits did not convince. The highest value achieved was about 27% with an input voltage of 1V and a current consumption of 2,5mA. The input voltage is near the startup voltage of the L6920, but it is still higher and the output is very low. The output voltage of 2,6V is too low to feed any power circuit, it may, however, be used to power other DC-DC converters but that will only add more consumed current to the equation, and therefore this is not a solution for this specific problem. May however be a solution for other harvesting technology that may have sufficient input power to be used.

6.2 Future Work

Since the experiments did not result in what we were expecting, some more research work will be needed, such as with more new technologies that can work with ultra low voltage and with low current consumption.

On the ultra low voltage Oscillator maybe the future works needs to optimize it to obtain a better square wave with a higher frequency that do not compromises the signal excursion, and implement a better switching MOSFET in the Pre-Boost Converter.

As for the Boost Converter, it seems that nothing else can be optimized. Maybe other boost techniques besides the ones presented here can be approached and the effects of a variable duty cycle in high loads studied. This way, the future work is the search for new boost techniques and the evaluation of different duty cycle effects in high loads.

Regarding the germanium circuits there is nothing to research, since they were very common in the 1950s and 1960s, and for that a lot of studies were done with them.

For the current consumption, it was realized this is the major inhibition to go around with future work. Maybe an ASIC, that stands for application-specific integrated circuit. A specific integrated circuit (IC) customized for a particular use, rather than intended for general-purpose use, could be a better solution. In this situation all the circuit components could be designed with specific measures in a way that could reduce the current consumption and losses, since all the components are in the same chip.

References

1. **Ji Wang, Stuart Gray, Donnell Walton and Luis Zenteno.** *Fiber fuse in high power optical fiber.* USA : s.n., 2008.

2. **Linear Technologies.** *DC-DC Converters for Portable Computers.* [Design Notes] Milpitas : Linear Technology Corporation, 1991.

3. **XP Power.** *DC-DC 1W IE Series.* [datasheet] s.l. : XP Power, 2009.

4. **Ned Mohan, Tore M. Undeland, William P. Robbins.** *Power Electronics.* Hoboken : John Wiley & Sons, Inc., 2003.

5. **Basso, Christophe.** *Switch Mode Power Supplies: SPICE Simulations and Practical Designs.* New-York : McGraw-Hill, 2008.

6. **International Telecommunication Union.** *Mobile Cellular , Subscriptions per 100 people.* Geneva, Switzerland : International Telecommunication Union, 2008.

7. **Hsieh-Hung Hsieh, Liang-Hung Lu.** *A High-Performance CMOS Voltage-Controlled Oscillator for Ultra Low Voltage Operations.* [Manuscript] Taiwan : s.n., 2006.

8. **Kim, Kyung Ki Kim and Yong-Bin.** *Ultra-Low Voltage High-Speed Schmitt trigger Circuit in SOI MOSFET technology.* [Paper] Boston, USA : IEICE Electronics Express, 2007.

9. **Dorward, John Ash and Richard.** *Market Trends in Optical Networks - the Service Drivers and Technology Impact.* United Kingdom : Ericsson Ltd., 2008.

10. **J. Prat, P. Chanclou and all SARDANA contributors.** *FTTH evolutions: The SARDANA Concept.* [Presentation] Brussels : MARKET FOCUS - ECOC, 2008.

11. **J. A. Lázaro, J. Prat, P. Chanclou, G. M. Tosi Beleffi, A. Teixeira, I. Tomkos, R Soila, V. Koratzinos.** *Scalable extended reach PON.* [paper] San Diego : OFC/NFOEC, 2008.

12. **Baptista, Albano Manuel Cardoso.** *Reconfigurable Remote Nodes for hybrid Passive Optical Networks.* Aveiro : Universidade de Aveiro, 2008.

13. **Chandrakasan, Rajeevan Amirtharajah and Anantha.** *Self-Powered Low Power Signal Processing.* Massachusetts : s.n., 1997. Vol. Symposium on VLSl Circuits Digest of Technical Papers.

14. **V. M. Pacheco, L. C. Freitas, J. B. Vieira Jr., E. A. A. Coelho and V. J. Farias.** *Stand-Alone Photovoltaic Energy Storage System With Maximum Power Point Tracking.* Uberlândia : IEEE, 2003.

15. **Loreto Mateu, Cosmin Codrea, N´estor Lucas, Markus Pollak and Peter Spies.** *Energy Harvesting for Wireless Communication Systems Using Thermogenerators.* 2006.

16. **Rudy P. Sevems, G. Ed Bloom.** *Modern DC-DC Switchmode Power Conversion Circuits.* s.l. : Van Nostrand Reinhold, 1985.

17. **Chryssis, George C.** *High Frequency Switching Power Supplies: Theory and Design.* s.l. : McGraw-Hill, 1989.

18. **Andre S. Kislovski, Richard Redl, Nathan O. Sokal.** *Dynamic Analysis of Switching-Mode DC/DC Converters.* s.l. : Van Nostrand Reinhold, 1991.

19. **Pressman, Abraham I.** *Switching Power Supply Design.* s.l. : McGraw-Hill, 1997.

20. **Analog Linear Devices.** *EH300/EH301 EPAD® Energy Harvesting Modules for Low Power Applications.* [Brochure] Sunnyvale, CA : ALD Inc., 2007.

21. **Mário Lima, António Teixeira.** *Receptores Ópticos.* [PDF] Aveiro : s.n., 2008/2009.

22. **Doherty, Bill.** *Micro Notes Series.* [PDF] Watertown : Microsemi.

23. **Raúl Sananes, Carlos Bock and Josep Prat.** *Techno-Economic Comparison of Optical Access Networks.* [Paper] Barcelona, Spain : ICTON 2005, 2005.

24. **A. Baptista, M. Ferreira, A. Quinta, M. Lima, A. Teixeira.** *Remotely Reconfigurable Remote Node for Hybrid Ring-Tree Passive Optical Networks.* [Paper] Portugal : Instituto de Telecomunicações, Universidade de Aveiro, 2008.

25. **H. Ramanitra, P. Chanclou, Z. Belfqih, M. Moignard, H. Le Bras and D. Schumacher.** *Scalable and Multi-service Passive Optical Access Infrastructure Using Variable Optical Splitters.* [Paper] France : NOA "Next Optical Access" Network, France Telecom Division R&D/RESA/GHOA, 2005.

26. **J.G. Werthen, A.G. Andersson, S.T. Weiss and H.O Bjorklund.** *Current measurements using optical power.* [Paper] s.l. : Transmission and Distribution Conference, 1996.

27. **Advanced Linear Devices.** *EH300 Brochure.* s.l. : ALD, Inc, 2007.

28. —. *EH300/EH301 EPAD Energy Harvesting Modules.* Sunnyvale : ALD, 2007.

29. **ST Microelectronics.** *L6920 Datasheet.* s.l. : ST Microelectronics, 2005.

30. **Texas Instruments.** *LOW INPUT VOLTAGE SYNCHRONOUS BOOST CONVERTER WITH 1.3A SWITCHES, TPS61200 Datasheet.* s.l. : TI, 2008.

31. **RLH.** RLH webpage. [Online] [Cited: May 20, 2009.] http://www.fiberopticlink.com/Industry_Solutions/High_Voltage.html.

32. **Advanced Linear Devices.** *New Design Concepts in Ultra Low Voltage and Nanopower Circuits with EPAD MOSFET Arrays.* Sunnyvale, California : Advanced Linear Devices, 2005.

33. —. www.aldinc.com. *ALD Inc. Web Page.* [Online] [Cited: Abril 24, 2009.] www.aldinc.com.

34. —. *ALD110800.* [Datasheet] Sunnyvale, California : Advanced Linear Devices, 2005.

35. **National Semiconductor.** *Datasheet LM555.* América : s.n., Julho 2006. 2.

36. **Texas Instruments.** *SN74AUC1G14.* [Datasheet] Dallas, Texas : Texas Intruments, 2007.

37. —. *SN74AUC1G17 Schmitt Trigger Buffer.* [Datasheet] Dallas, Texas : Texas Instruments, 2003.

38. dev.emcelettronica. *dev.emcelettronica.com.* [Online] [Cited: May 29, 2009.] http://dev.emcelettronica.com/transistor-techniques-transistor-measurements.

39. **Yongseok Choi, Student Member, IEEE, Naehyuck Chang, Senior Member, IEEE, and Taewhan Kim, Member, IEEE.** *DC-DC Converter-Aware Power Management for Low-Power Embedded Systems.* s.l. : IEEE, 2007. Vol. 26.

Attachments

Printed Circuit Boards

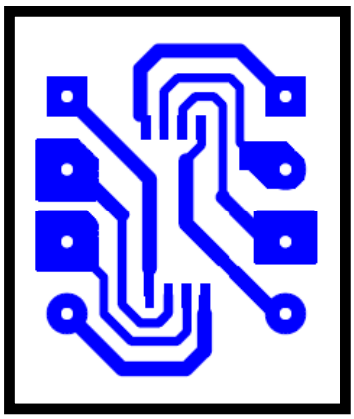

Attachment 1 - ST L6920 TSSOP8 - Package - Scale 5:1

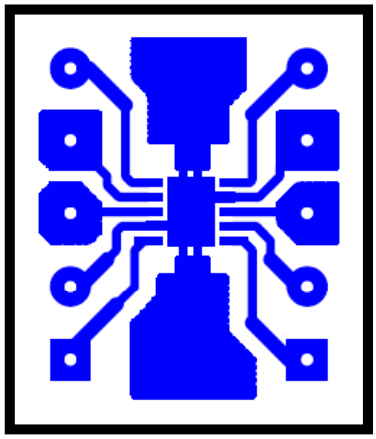

Attachment 2 - Texas Instruments TPS61200 - DRC (S-PVSON-N10) Package - Scale 5:1

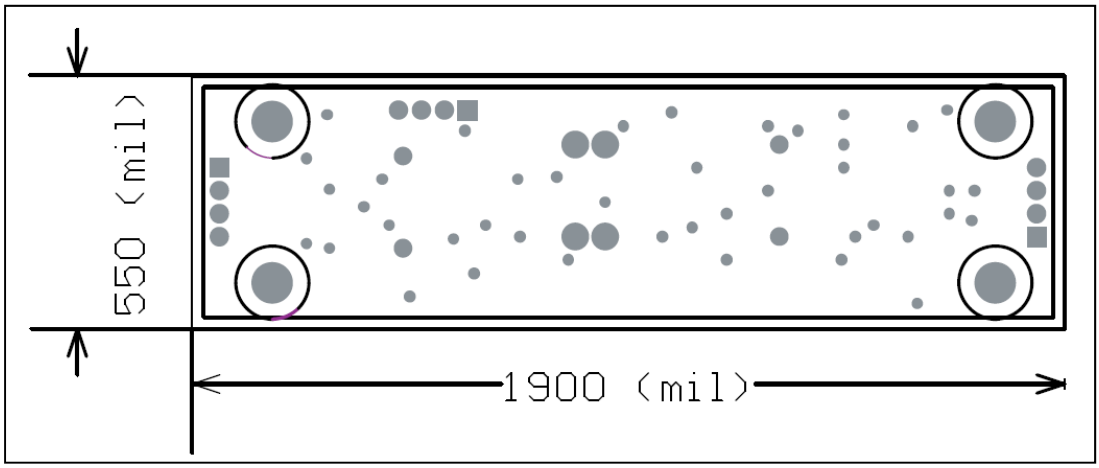

Attachment 3 - ALD Harvesting Module Dimensions

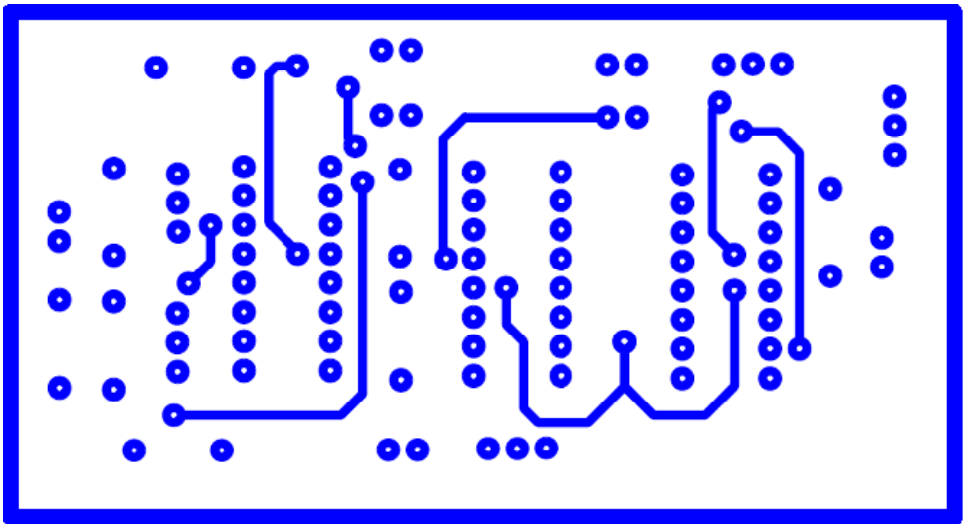

Attachment 4 – TOP Side of Oscillator with buffer and Pre-Boost Board - Scale 2:1

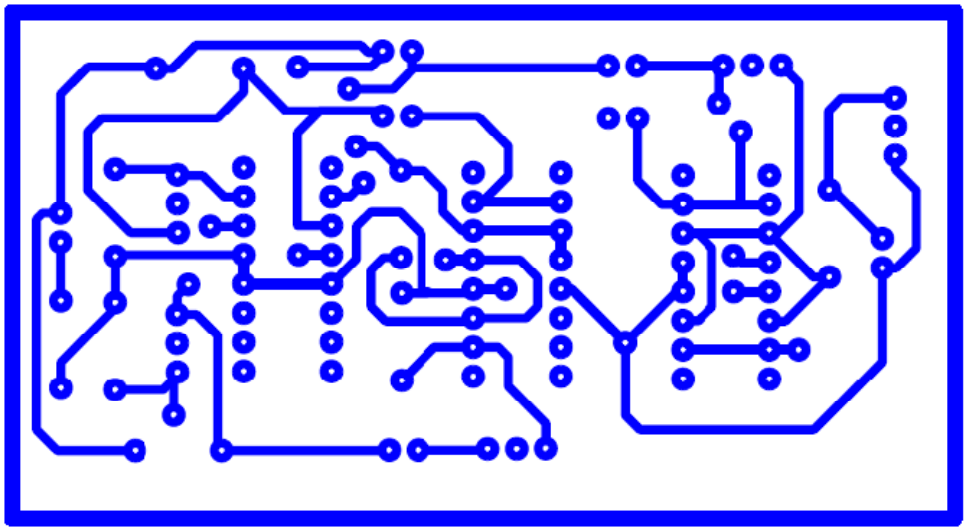

Attachment 5 - BOTTOM Side of Oscillator with Buffer and Pre-Boost

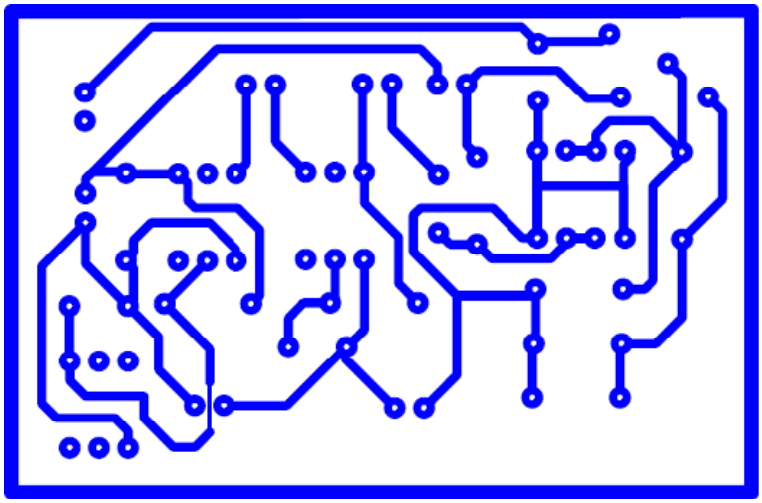

Attachment 6 - BOTTOM Side of Shmitt Triggers and Power MOSFET Board - Scale 2:1